

Article

Minute-Scale Forecasting of Wind Power - Results from the collaborative workshop of IEA Wind Task 32 and 36

Ines Würth ^{1*}, Laura Valldecabres ², Elliot Simon ³, Corinna Möhrlen ⁴, Bahri Uzunoğlu ⁵, Ciaran Gilbert ⁶, Gregor Giebel ³, David Schlipf ⁷, and Anton Kaifel ⁸

¹ Stuttgart Wind Energy, University of Stuttgart, Allmandring 5b, 70569 Stuttgart, Germany; wuerth@ifb.uni-stuttgart.de

² ForWind - University of Oldenburg, Institute of Physics, Küpkersweg 70, 26129 Oldenburg, Germany; laura.valldecabres@forwind.de

³ DTU Wind Energy (Risø Campus), Technical University of Denmark, Frederiksborgvej 399, 4000 Roskilde, Denmark; ellsim@dtu.dk, grgi@dtu.dk

⁴ WEPROG, Eschenweg 8, 71155 Altdorf/Böblingen, Germany, Willemoesgade 15B, 5610 Assens, Denmark; com@weprog.com

⁵ Dept. of Engineering Sciences, Division of Electricity, Uppsala University, The Ångström Laboratory, Box 534, 751 21 Uppsala, Sweden; Dept. of Mathematics, Florida State University, Tallahassee, FL, USA, 32310; bahriuzunoglu@computationalrenewables.com

⁶ Department of Electronic and Electrical Engineering, University of Strathclyde, 204 George St, Glasgow G11XW, UK; ciaran.gilbert@strath.ac.uk

⁷ Wind Energy Technology Institute, Hochschule Flensburg, Kanzleistraße 91–93, 24943 Flensburg, Germany; david.schlipf@hs-flensburg.de

⁸ Zentrum für Sonnenenergie- und Wasserstoff-Forschung Baden-Württemberg, Meitnerstraße 1, 70563 Stuttgart, Germany; anton.kaifel@zsw-bw.de

* Correspondence: wuerth@ifb.uni-stuttgart.de; Tel.: +49-711-685-68285

Academic Editor: Emanuele Ogliari, Sonia Leva

Version January 31, 2019 submitted to Energies

Abstract: The demand for minute-scale forecasts of wind power is continuously increasing with the growing penetration of renewable energy into the power grid, as grid operators need to ensure grid stability in the presence of variable power generation. For this reason, IEA Wind Tasks 32 and 36 together organized a workshop on “Very Short-Term Forecasting of Wind Power” in 2018 to discuss different approaches for the implementation of minute-scale forecasts into the power industry. IEA Wind is an international platform for the research community and industry. Task 32 tries to identify and mitigate barriers to the use of lidars in wind energy applications, while IEA Wind Task 36 focuses on improving the value of wind energy forecasts to the wind energy industry. The workshop identified three applications that need minute-scale forecasts: (1) wind turbine and wind farm control, (2) grid power balancing, (3) energy trading and ancillary services. The forecasting horizons for these applications range from around 1 s for turbine control to 60 minutes for energy market and grid control applications. The methods that can be applied to generate minute-scale forecasts rely on upstream data from remote sensing devices such as scanning lidars or radars, or are based on point measurements from met masts, turbines or profiling remote sensing devices. Upstream data needs to be propagated with advection models and point measurements can either be used in statistical time series models or assimilated into physical models. All methods have advantages but also shortcomings. The workshop’s main conclusions were that there is a need for more research into new minute-scale forecasting techniques and that more efforts should be directed towards enhancing quality and reliability of the forecasts. On the long term, standards are required to support the adoption of these methods.

21 **Keywords:** wind energy; minute-scale forecasting; forecasting horizon; Doppler lidar; Doppler radar;
22 numerical weather prediction models

23 **1. Introduction**

24 In the past years, minute-scale forecasting of wind power has become an important research
25 topic in the wind energy community. Whereas traditional forecasting techniques provide a forecasting
26 horizon in the hour or day range [1], new methods allow to predict the power output of wind turbines
27 or wind farms on a minute scale. Due to the increasing penetration of renewable energy power systems
28 into the grid, there is a demand for minute-scale wind power forecasts, as grid operators need to
29 ensure grid stability in spite of the highly fluctuating power sources. The forecasts become even more
30 important with increasing sizes of wind farms of several 100 MW and especially if those wind farms
31 conglomerate geographically as it is the case for offshore sites. The objective of this paper is to provide
32 a summary of the needs of minute-scale forecasting and an overview of the developed methods and
33 the possible solutions to the barriers that prevent end users from adopting them.

34 The results presented in this paper are based on the outcome of the collaborative IEA Wind Task
35 32 and 36 workshop “Very Short-Term Forecasting of Wind Power” held in Roskilde, Denmark in June
36 2018. IEA Wind Task 32: “Wind Lidar Systems for Wind Energy Deployment” is an international open
37 platform with the objective of bringing together experts from the academic and industrial communities
38 to identify and mitigate barriers to the use of lidar for wind energy applications. IEA Wind Task 36:
39 “Forecasting of Wind Power” is focused on improving the value of wind energy forecasts to the wind
40 energy industry. During the workshop, 39 participants from academia, forecasting service providers,
41 wind farm operators as well as the lidar and wind turbine manufacturers discussed the future needs of
42 minute-scale forecasting, the advantages and barriers of different forecasting techniques and strategies
43 for overcoming those barriers.

44 This paper is organized as follows. Section 2 discusses the need for minute-scale forecasting
45 and explains target forecasting horizons for different applications. In Section 4, different forecasting
46 techniques are described. To that end, first a review of state-of-the art forecasting techniques and the
47 gap that needs to be closed with new methods in order to achieve minute-scale forecasts is given. Then
48 different approaches to close the gap are discussed and for each method barriers and possible solutions
49 are given. In Section 6 challenges for the implementation and commercialization of the new methods
50 are discussed and the paper is finalized with conclusions in Section 7.

51 **2. Intra-hour variability of wind power generation**

52 In 2017 Denmark was the country with the highest wind power penetration rate (44% of the
53 annual consumption of electricity), followed by Portugal (24%) and Ireland (24%). In the case of
54 Denmark, the maximum hourly penetration rate was over 140%. With a total net installed capacity of
55 169 GW, the power generation capacity of wind power in Europe increased by almost 300% in the last
56 10 years [2]. Given the expected rising penetration levels of wind power and the increasing size of on-
57 and especially offshore wind farms feeding power into the grid at a single point [3], it becomes crucial
58 to have more precise forecasts of wind power generation with lead times of few minutes ahead and
59 temporal resolutions of seconds or minutes.

60 When generating a forecast, one useful practice is to consider the power spectral density (PSD)
61 of the measured physical process to understand which time frequencies contribute to the variance
62 of the signal. Peaks in the spectra correspond to larger relative fluctuations which are traditionally
63 more difficult to capture and predict. This type of analysis is demonstrated in Larsen et. al [4] using
64 long-term site measurements from Høvsøre test station and Horns Rev offshore wind farm in Denmark.
65 Boundary layer wind spectra were resolved across cycles ranging from 0.1 seconds (10 Hz) to 1 year.
66 Figure 1 presents a main result of that work which compares full scale wind PSDs at 50 m height both

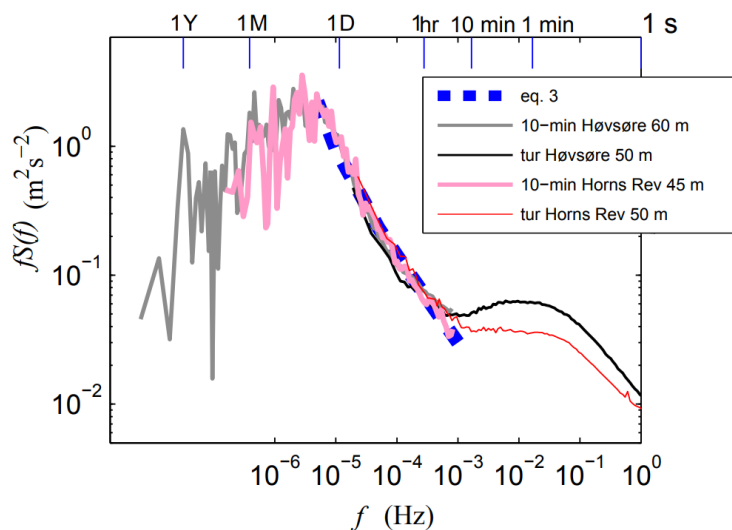


Figure 1. Power spectral density (PSD) of wind speed with corresponding timescales denoted atop. High frequency sonic measurements are used to devise the onshore (black) and offshore (red) lines. Reproduced with modifications from Larsen et. al [4] with permission from the Springer Nature publisher.

67 on- and offshore [4]. Apt [5] presents a similar PSD analysis of wind turbine output using 1-second
 68 power data for a single wind turbine as well as a 6-turbine wind farm. Attributes of the PSD signal
 69 will vary by location, time, sensor type, and physical property being measured. Still, from the results
 70 in Figure 1, a strong local peak can be detected around 1 min, indicating the strong variability of the
 71 wind at that temporal scale. This variability of the wind is associated to atmospheric phenomena like
 72 open cellular convection, gravity waves, sea breezes or low level jets, among others [6]. At frequencies
 73 $f > 0.02$ Hz, i.e. periods below one minute, the PSD signal strongly decreases and, as reported in [7],
 74 wind power fluctuations of large wind farms are not considered an issue due to the smoothing effect
 75 of aggregated power.

76 Yet, the intra-hour variability of wind power not only depends on the variability of the wind itself
 77 but on the size of the wind farm, the number of wind turbines and their geographic dispersion. Indeed,
 78 it has been shown by several authors that for offshore wind farms, the small geographic dispersion of
 79 the wind turbines results in an increased power variability in the minute scale, compared to widely
 80 dispersed onshore wind turbines [8].

81 The enhanced variability in those time scales leads to rapid changes in wind power generation
 82 (ramp events). These unexpected events are mainly caused by extreme changes in wind speed and/or
 83 direction in a very short period of time, and are frequently associated with the passage of weather
 84 fronts. Despite being critical for the management of the grid, the dynamic allocation of reserves and the
 85 stability of the system [9,10] there is no standard definition of a ramp event. Indeed, it is an individual
 86 process of the end-user to define critical ramps and thereby ramp events. A recent publication on
 87 the history of wind power ramp forecasting [11] gives an overview of the definitions used in ramp
 88 event detection, the meteorological conditions associated to those events and the current forecasting
 89 techniques. For most wind power forecasting applications however, the definition of what is critical for
 90 an end-user is very individual and dependent on the application as well as the available reserves. For
 91 example, a system operator on an island grid or badly interconnected grid needs to have all reserves
 92 available within the control zone in order to prevent that a critical ramp could cause security issues. A
 93 trader may also be very interested in ramp forecasts, as just one event with a large error may cause
 94 95% of the imbalance costs in a month.

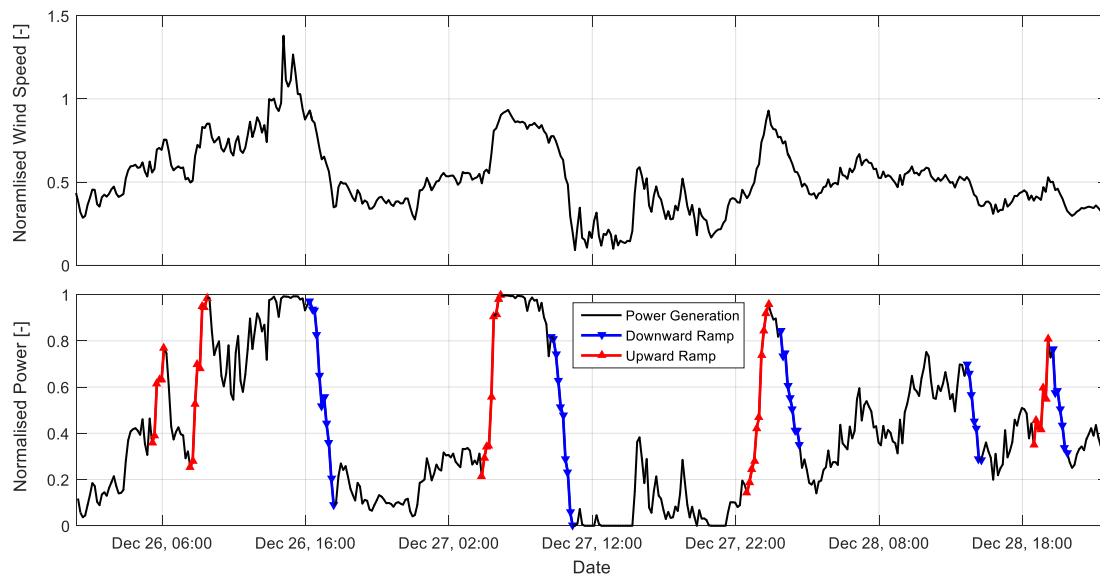


Figure 2. Example time series of wind speed and generated power of a single wind turbine with wind ramps marked for a time window of 60 min and a change of power of 40%. The time series is based on 10-minute averages. Reproduced without modifications from Würth et al. [12] with permission <https://creativecommons.org/licenses/by/3.0/>.

Ramp events are often classified into ramp-up and ramp-down events, according to the direction of the power gradient. As an example, the time-series in Figure 2 illustrates a number of steep ramps in both directions. While ramp-up events always can be handled in the very short term with curtailments, ramp-down events can become extremely critical due to the sudden missing generation. This enhances the importance of generating accurate minute-scale forecasts of wind power.

3. An overview of different applications for minute-scale forecasting in the wind industry

The forecast horizon and the parameters that are needed to be forecasted, depend on the application of the forecast. Three applications have been identified where minute-scale forecasts of wind speed or power are needed.

1. **Wind farm control:** Wind turbine and wind plant controllers need the information to optimize e.g. the power output of the turbines.
2. **Physical balancing:** They are required by the Transmission System Operator (TSO) in order to optimally operate reserves for the continuous balance of the power system and grid constraint management.
3. **Economic balancing:** Trading and balancing of wind power in the intra-day or rolling power markets require minute-scale updates of the forecasts with real power output in order to reduce imbalance costs and increase incomes.

It is expected that a next step in the evolution will be storage system planning and optimization in the real-time markets, where the bulk of the energy production will come from renewable energy sources. However, this paper focuses on the applications listed above. In the following each application is discussed in more detail.

3.1. Wind turbine and wind farm control

Preview information of the wind field is helpful for the control of wind turbines and wind plants. Wind turbines are highly dynamic systems that are excited by stochastic influences from the

wind and most of the wind turbine control is designed to deal with variations in this disturbance. However, traditional feedback controllers are only able to react to impacts of wind changes on the turbine dynamics after these impacts have already occurred. Lidar-assisted control algorithms, which can exploit preview information of the wind, are promising to provide improved operation over conventional control algorithms, with the ultimate aim of increasing the energy yield while keeping the structural loads low. Regarding the required preview time, the following classification is useful:

1. around 1 s: Feedforward control is used to compensate wind changes to reduce structural loads. For e.g. the blade pitch, the rotor-effective wind speed is needed only a short time before the wind reaches the rotor to overcome the pitch actuator dynamics.
2. around 5 s: For Model Predictive Control, the control inputs are optimized to get a chosen compromise of load reduction, energy production, and actuator wear [13]. Here, a short time horizon of wind characteristics such as wind speed, direction, and shear is used, typically 5-10 s.
3. around 1-10 min: For yaw control, a wind direction estimation is used to align the wind turbine with the mean wind direction. For this, a preview in the minute scale is helpful.

Active wind farm control is a promising technology to increase the energy production of wind farms [14]. However, flow models are still an important research topic, and the validation of flow models and control strategies is still ongoing. Wind preview for flow control is mainly used for induction control and wake steering for higher energy capture and management of fatigue loading. Regarding the required preview time, following classification is useful:

1. around 10 sec to 1 min for induction control: Usually the blade pitch angle is used to reduce the power and thrust to weaken wake effects on downstream turbines, which increase the overall production. At partial load this is done by adjusting the “fine pitch” settings which is usually based on a filtered wind speed estimate. Wind preview might help to better adjust the power balancing.
2. around 1-10 min for wake steering: The yaw misalignment is used to deflect wakes away from downstream turbines and thus similar preview times compared to the conventional yaw control is useful. A preview of the wind direction might help to better adjust the unintended yaw misalignments in a wind farm.

3.2. Power grid balancing, frequency control and power quality in reserve market

The focus in this section is on grid balancing, frequency control and power quality embedded in reserve market while the energy market and ancillary services are discussed in the following Section 3.3. The balancing term can be employed in a much broader sense in the context of balancing longer time scales. However in these time scales of mainly energy and reserve market, where balancing actions are scheduled before the real time, there are several other means of observations with lower resolutions available. [15–17]. However, these are not in the time scales of minute-scale forecasting that is the focus of this section. It should be noted that there are differences in terminology in different countries for same and slightly different balancing actions. In this section, the EU terminology is adopted for the rest of the discussions.

To guarantee the stability of the grid, supply and demand always have to be balanced in spite of the fluctuating power sources. Power quality is achieved if the grid frequency stays within a certain range of a rated value. An imbalance between supply and demand impacts voltage stability and grid frequency, hence there is a need for power balancing [15,18–20].

The volatility of wind resources creates volatility in the supply and as a result, balancing control actions are needed. One can distinguish between different time scales in this phase of controls embedded in the reserve market, which are known as primary, secondary, and tertiary control. The autonomous response of the system to supply/demand imbalances is automatically addressed with primary controls, which is in the scale of microseconds to seconds. In the secondary controls, there are automatic actions and manual actions in scales of seconds to minutes. In the tertiary controls, both

167 manual and automatic controls are in action from minutes to quarter of an hour to half an hour scale.
168 All of these actions of balancing are carried out in order to ensure power system quality. Any forecast
169 data that is available in scale of microseconds to minutes can be automatically employed in the state
170 estimator of the controller [15,18–20]. The state estimator corrects with observational data, the state of
171 the system.

172 From the market point of view, primary and/or secondary controls do not involve auction
173 mechanisms. The participation to primary and secondary control can be traded by auction. This results
174 in the availability of reserve for primary and/or secondary control. The market period can be day
175 to year. The reserve market addressed in the context of primary and/or secondary controls consists
176 of generators that can allocate themselves to be available as reserves for primary and/or secondary
177 control. This availability is for a predefined time period for automatic control. This is achieved without
178 any bidding as a result of commercial agreements or participation based on the context of the country.
179 If there is utilization of reserve service, an utilization price is employed based on [21].

180 Wind power and other renewable energy create low levels of rotational inertia since these energy
181 conversion systems do not normally act on rotational inertia which has impacts on the power grid
182 frequency. Moreover asynchronous machines and Double Fed Induction Generator (DFIG) are
183 disconnected by inverter from rotating mass of inertia. Suppliers have started to make changes
184 to create synthetic inertia that can emulate inertia synthetically [22]. Synthetic inertia is about acting to
185 AC frequency, possibly after the loss of a big power plant which makes the grid under-supplied and
186 will result with the AC frequency beginning to fall. This makes the accurate short-term forecasting
187 even more important since all of these emulations are dependent on accurate estimation of wind
188 speeds. Hence automatic control for primary and/or secondary controls will certainly benefit from
189 more accurate forecasting on the short-time scales of minutes in control applications.

190 3.3. Energy and ancillary services markets

191 Electricity markets need to be balanced in order to match the supply and demand of energy. This
192 physical balancing of the transmission grid is carried out by the transmission system operators (TSO)
193 or by an independent system operator (ISO). Given the increased integration of power generation from
194 variable sources of energy like wind and solar, the physical balancing has become more complicated.
195 Therefore, electricity markets with such intermittent and variable sources have to become more flexible
196 and introduce either rolling markets (e.g. in the UK and Australia) or introduce shorter intra-day
197 auctions, additional to the day-ahead auction, which have become very popular in Europe. Among
198 the intra-day market platforms, one can distinguish between discrete auctions or continuous intra-day
199 markets. In intra-day auction markets like in Italy, Spain or Portugal, intra-day bids are restricted
200 to a few established auctions. By contrast, in continuous intra-day markets, counter parties match
201 the bids using a trading platform that operates continuously. Those continuous intra-day balancing
202 markets operate in Europe with different lead times ranging from 5 to over 100 minutes and most of
203 the countries work with trading blocks of 15 minutes. Table 1 includes the lead times and smallest
204 trading blocks for several countries in Europe and for Turkey. A more detailed description of the
205 electricity markets and their time lines can be found in [23]. Hence, the importance of the use of
206 updated available minute-scale forecast of wind power has arrived to stay.

Table 1. Lead times and smallest trading blocks for different countries. Sources: Epex [24], Nordpool [25], EXIST [26], and BSP South Pool [27].

Country	Lead time (minutes)	Trading blocks (minutes)	Market
Austria and Germany	5	15	EPEX Spot
Bulgaria, Denmark, Estonia, Finland, Lithuania, Norway and Sweden	60	15	NordPool
Belgium, France and the Netherlands	5	60	EPEX Spot
Slovenia	60	15	BSP Southpool
Switzerland	30	15	EPEX Spot
Turkey	90	60	EXIST

207 In light of this, the forecast process can be split into three components: (1) production of a smooth
 208 day-ahead forecast tuned for economic adjustment via the intra-day market, (2) targeting intra-day
 209 forecasts for the predictable part of the day-ahead forecast errors and (3) application of forecasts
 210 on minute-scale to manage the wind after gate closure of the intra-day. The two first components
 211 correspond to current practices in long-term and short-term processes with some enhancements. The
 212 third component is a process running on minute-scale with 1 or 2 hour look ahead [e.g. 28].

213 Minute-scale forecasts are also necessary when applying to provide ancillary services, secondary
 214 or tertiary reserve or balancing capacity for the pool of large utilities. For instance, a recent pilot project
 215 in Germany allows wind power generators to participate in the reserve market by down-regulating
 216 their production. The possible or available power produced by the wind farms needs to be calculated
 217 in one-minute intervals. Furthermore, the standard deviation of the percentage error of the possible or
 218 available wind farm power, during the pilot phase, should be less than 5% [29].

219 4. State-of-the-art of wind power forecasting

220 State of the art wind power forecasting methodologies utilise wind speeds from weather forecasts
 221 and on-site real-time measurements to compute wind power.

222 Figure 3 shows qualitatively the forecast error levels of a day-ahead, hours-ahead and
 223 minutes-ahead forecast compared to a persistence error, where the persistence forecast is the most
 224 recent available measurement. The qualitative visualisation of the forecast errors in the different
 225 time scales shall be seen in the light of their starting point and forecast error growth over time. For
 226 example the day-ahead forecast has an almost linear error growth and is typically responsible for
 227 approximately 1/3 of the forecast error [30]. The day-ahead forecast also starts with an inherent error
 228 at forecast time zero due to a number of aspects. In [30] these are described as for example (i) the
 229 initial weather conditions; (ii) sub grid scale weather activity; (iii) coordinate transformations; (iv) the
 230 algorithm used to compute the wind power; (v) imperfection of turbines and measurement errors.
 231 For Pahlow et al. [30] one question remained: which fraction of this background error is caused by
 232 imperfect initial conditions of the weather forecast and which fraction is due to erroneous wind power
 233 parameterizations. They extrapolated the linear forecast error growth from 9-45 hours down to the
 234 0 hour forecast and thereby estimated the background mean absolute error (MAE) just under 4% of
 235 installed capacity. Part of of that gap of approximately 4% error at initial time can be reduced by the
 236 hours ahead forecast with knowledge about the real power production. Pahlow et al. [30] characterised
 237 this inherent error at the initial time to a mix of unknown technical and non-technical constraints at
 238 the forecast location. These can be wind farm specific constraints, such as unknown non-availability of
 239 wind turbines, but also errors due to the computation of the wind power at the site. The hours-ahead
 240 forecast are steeper in it's error growth than the day-ahead and reaches this level typically around
 241 4-8 hours ahead in time. This time span is the typical temporal influence radius of a measurement
 242 [30]. The minute-scale and persistence forecasts are both starting at the zero error in their initialisation.
 243 This is what characterises this forecasting time scale, where the current state of the power plant is

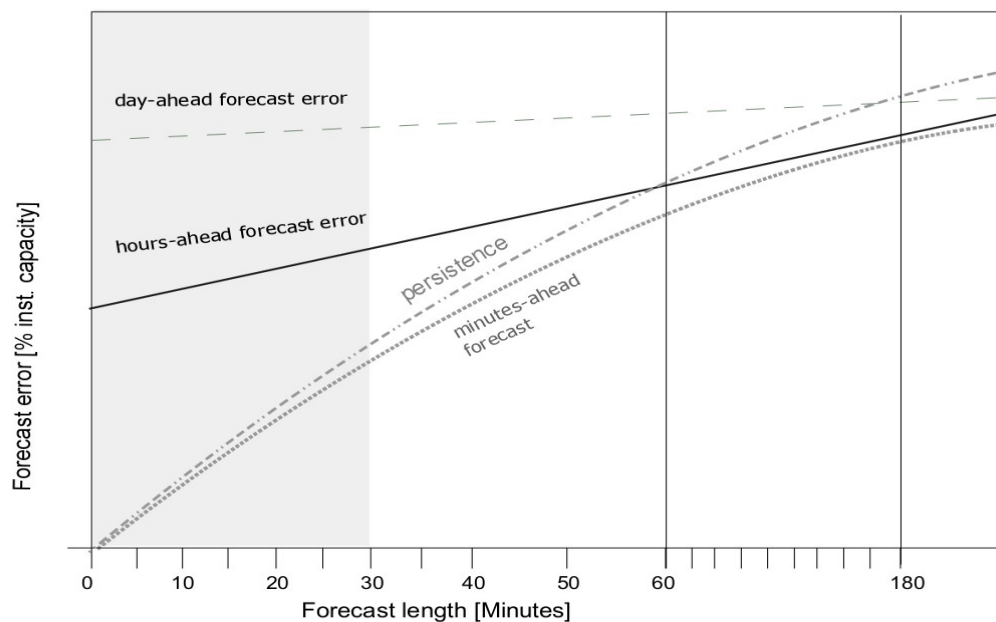


Figure 3. Qualitative visualisation of the forecast error development over the first hours of a forecast for different temporal forecast techniques.

fully known. The steepness of the error is also highest for these two forecast techniques due to the decrease of influence of the measurement at the power plant over time. A general industry experience is that a persistence forecast is at the same level as a hour-ahead forecast after around one hour. A minute-ahead forecast should ideally be below the hour-ahead forecast for about 3 hours as a thumb rule when evaluating the usefulness of the technique. The time between 1 hour and 3 hours into the forecast is where the persistence forecast typically reaches the day-ahead forecast error level and loses forecast skill.

Figure 3 illustrated nicely that the margin of possible improvements by minutes-ahead forecasts in the first 30 minutes of the forecast is rather small in comparison to persistence. Additionally, the average error growth of up to 2% of the installed capacity of a short-term forecast of 15 minute time resolution is rather steep (see Figure 3). It is therefore fair to say that the improvement over persistence, which is the objective in the very short time ranges of minutes and hours, is therefore rather modest. This is often used as a reason not to base decisions on forecasts, but rather use persistence, even during ramping, where the persistence forecast is a poor approximation. If the previous 15-minute forecast already appears to be off track, then the forecast user cannot justify to trust in the forecast. Also, the similarity between the average error of a short-term forecast and persistence over the next 15 minutes strongly indicates whether the short-term forecast has good or less good quality.

Forecast providers are continuously looking for enhancements, which can improve the hour-ahead and minute-scale forecast in the less good quality periods, because these result in the most significant power system benefits. Use of wind speed measurements in addition to wind power measurements is therefore a key to improve forecasts in periods, where the wind speed is in the flat ranges of the power curve ($< 5 \text{ m/s}$ or $> 12 \text{ m/s}$). Without wind speed measurements, the minute-scale forecast is in fact unable to correct the weather forecast for phase errors in periods, where the generation is zero or at full capacity.

A steady increase in wind speed from 15 m/s to above the high-speed shutdown point at 25 m/s can also be improved by using wind speed measurements in the short-term algorithms. At the high-speed shutdown points ($> 25 \text{ m/s}$), the wind speed forecast uncertainty is at least 2 m/s even

271 in high predictability events. The timing of the shutdown is therefore uncertain, even a few minutes
272 before it happens. Wind speed measurements from the wind farms reduce this uncertainty significantly.
273 The timing of the high speed shutdown is important for grid security, because there are potentially
274 many Megawatts instantly ramping down. In combination with forecasting on the minute-scale,
275 such wind speed measurements can help to bridge the gap between the actual generation and both
276 short-term and long-term forecast.

277 For wind speeds below the cut-in level there are similar considerations. Mostly, a cut-in wind
278 speed occurs at a low aggregated wind power generation. Nevertheless, a large and strong low
279 pressure centre may have near zero wind speeds from different directions. Both, the changes in
280 wind direction and wind speed are better identified by wind speed measurements than wind power
281 measurements. Thus, information about wind speeds below cut-in can be crucial for the forecast
282 accuracy near a low pressure system centre at high aggregated wind power generation. During periods
283 of moderate and high generation, wind speed measurements can be used to calculate current turbine
284 availability or validate the delivered availability value. To conclude, measurements of low, medium
285 and high wind speeds all add value to forecasting, while those measurement signals in the steep range
286 of the power curve are least important.

287 From a technical perspective of the instrumentation, one of the most reported gaps for forecasting
288 hours-ahead and minutes-ahead is the quality of the measurement signals. While wind farm developers
289 have to use calibrated instrumentation and standardized methodologies in order to obtain a bankable
290 level of siting accuracy in the first phase of a wind project, i.e. the planning and commissioning phase,
291 the use of meteorological measurements is mostly not or badly defined, documented nor standardized
292 in the following operational phase. Although the measurements are important in many ways, e.g.
293 situational awareness in extreme events, scheduling and dispatch of generation on power system
294 level, the balancing of large forecast errors, maintenance of instrumentation, there are no standards
295 for the quality of the signals in real-time environments today. For example, if a measurement stops
296 working correctly and sends constant values, a persistence forecast will benefit in a verification, while
297 the forecast is penalized for providing a more realistic view of the situation. Dependent on the amount
298 of such periods with constant values, this can easily lead to an overestimation of the performance of a
299 persistence forecast in comparison to minutes-ahead forecasts and thereby prevent use and application
300 of minutes-ahead forecasts.

301 Due to such missing standards and industry guidelines, the main gaps for the use of and collection
302 of meteorological measurements and thereby advances in minute-scale forecasting can be summarized
303 as:

- 304 • lack of requirements in the grid codes
305 • lack of strategy for handling of missing or constant signals from measurements in real-time
306 • lack of quality of measurements in real-time

307 5. Review of methods for minute-scale forecasting

308 In the previous section we discussed the state of the art in minute-scale forecasting. In this section
309 we investigate instrumentation that can improve forecasting with current techniques and we outline
310 which and how new types of instrumentation can be used to improve forecasting on minute scale
311 when persistence does no longer provide a correct picture of the weather conditions.

312 5.1. Minute scale forecasting based on preview data from remote sensing devices

313 Remote sensing techniques are a new technology development in wind energy applications,
314 which has its roots in the desire to find alternative measurements for expensive and at times difficult
315 installation and erection of met masts. Especially with increasing hub heights, met mast heights have
316 grown to a dimension, where the erection requires planning permission and cranes of significant size.
317 Hence, it has become so expensive that previously never considered alternatives from the remote
318 sensing area have become price competitive. An additional compelling justification is that the cost of

319 lidar instruments have fallen significantly over the same time, driven in tandem by competition and
320 the telecommunications boom, which has resulted in affordable optical fiber components becoming
321 available.

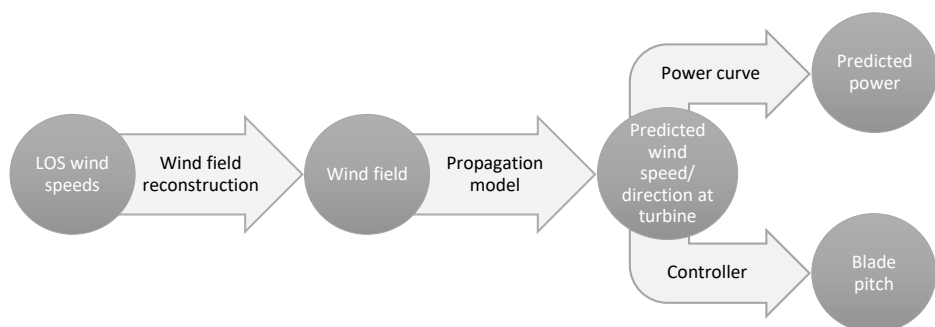
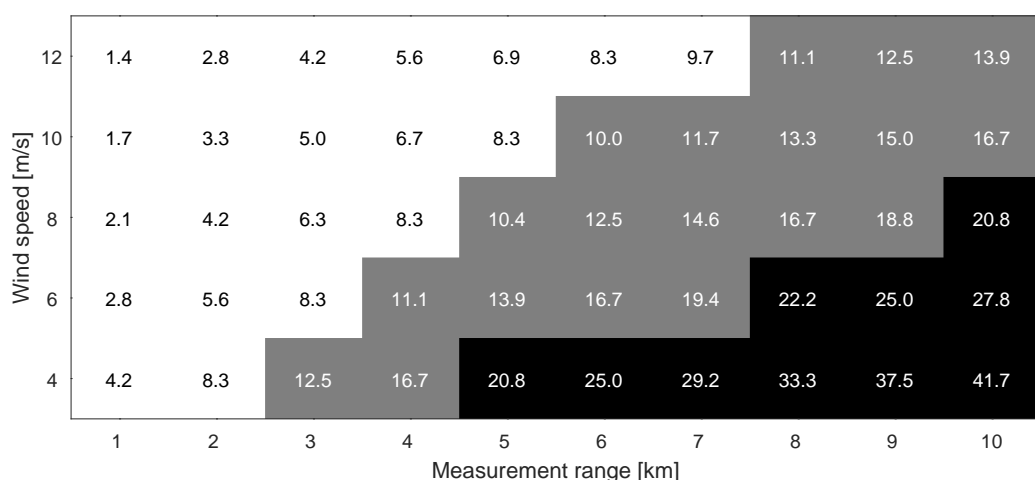
322 The main driver of recent developments has been the competitiveness in price, the ease of
323 installation and the increasing heights of wind turbines and size of the projects, where it is often no
324 longer sufficient to measure at only one site. Nevertheless, the disadvantage of not directly measuring
325 the target value is still present, as remote sensing devices only measure the wind speed in direction of
326 the emitted beam. With increasing experience and technical advances in technology, the remote sensing
327 devices have however become a real alternative. This has also been reflected in the IEC 61400-12-1
328 2017 standard [31], where such devices have been incorporated as possible instruments to carry out
329 wind measurements for wind energy applications. A new application for remote sensing devices is
330 forecasting. Especially scanning devices such as scanning lidars and radars offer the possibility to
331 carry out minute-scale forecasts by delivering high resolution temporal and spacial previews of the
332 upstream wind field of a wind turbine or wind farm. Therefore, the next two sub sections give an
333 overview of using those devices for forecasting purposes and finally lessons learned with remote
334 sensing instruments in real-time forecasting projects are summarized.

335 5.1.1. Scanning lidar-based forecasts

336 Wind lidars can measure the line of sight (LOS) wind speed at distances from a few centimeters to
337 several kilometers [32]. The first commercial wind lidar systems targeted at wind energy applications
338 appeared in the early 2000's [33]. Because of their costs and ease of installation, lidars have become
339 accepted as an alternative to the traditional mast-based wind sensors for site assessment and power
340 performance testing, as evidenced by their inclusion in international standards [31]. Additionally,
341 because they can measure upwind of operating turbines, wind lidars are used for feed-forward control
342 of wind turbines [34]. For this application nacelle-based lidar systems are used to measure the wind
343 speed several hundred meters upwind, thus forecasting the rotor effective wind speed seconds before
344 it hits the rotor just in time to pitch the rotor blades and reduce loads. A new application for scanning
345 lidars is wind power forecasting for power grid balancing. Commercial lidar manufacturers increased
346 the range of their systems and pulsed compact scanning wind lidars may now measure up to 10 km
347 away, enabling measurements across an entire site from one location [see e.g., 35,36]. The basic idea is
348 to use the spacial and temporal high resolution wind field information measured several kilometers
349 upwind of a wind turbine or wind farm to forecast the power output ahead in time.

350 The forecast process (Figure 4) is the same for both applications- control and power grid balancing.
351 First the raw lidar data is filtered for outliers and the horizontal wind speed and direction is
352 reconstructed from the measured LOS wind speeds. Depending on the number of synchronized
353 lidar measurements, different assumptions need to be made in order to resolve both horizontal wind
354 speed and direction. For instance, a velocity-azimuth display (VAD) retrieval technique is used to
355 resolve both wind speed and direction when only one lidar measurement is available [37]. Then
356 the wind speed in the distance is propagated towards the wind turbine by means of a propagation
357 model. The simplest model is based on Taylor's hypothesis which claims that turbulent eddies are
358 transported with the mean flow and do not change their properties. With this assumption the time can
359 be calculated that the wind speed measured in a certain distance needs to reach the turbine or wind
360 farm. Thus the farthest measured distance determines the forecast horizon. The forecasted wind speed
361 at the turbine or farm location is then used either to forecast the power output by means of a power
362 curve or as an input to the wind turbine controller.

363 As mentioned, the forecast horizon is determined by the measurement distance of the lidar and
364 the magnitude of the wind speed (Figure 5). For wind speeds at rated wind speed of a typical turbine,
365 the maximum forecast horizon with a state-of-the-art long-range scanning lidar that ideally measures
366 up to 10 km is around 15 min. The maximum horizon increases to around 40 minutes for a wind speed
367 of 4 m/s that corresponds to a typical cut-in wind speed.

**Figure 4.** Forecast process using lidar data.**Figure 5.** Forecast- horizon based on Taylor for different wind speeds and measurement ranges; horizon given in minutes; white: <10 min, grey: 10-20 min, black: >20 min [38].

The advantage of scanning lidars is that they offer the possibility to directly measure the wind speed upstream of a turbine. All the long-range scanning lidars are pulsed devices, which means that the wind speed information is gathered simultaneously at different measurement distances. Thus the wind flow can be tracked over the span of the measurement and local changes in the wind speed are captured. Modern lidars have compact dimensions of around one cubic meter which allows for flexible measurement campaigns and the installation for instance on the nacelle of a wind turbine or other alleviated points such as an offshore substation. Then the scanning of the area on e.g. a horizontal arc leads to the desired horizontal wind speed information after reconstruction without having to take into account shear effects.

Recent investigations have shown that lidar-based forecasting models were able to predict near-coastal winds better than the benchmarks persistence and ARIMA for a forecasting horizon of 5 min [39]. Another relevant study is Simon et al. (2018) [40] which explores space-time correlations of upwind lidar observations measured on a flat horizontal plane. The study also shows results of a 1–60 minutes ahead forecast method utilizing the lidar inflow scans which significantly outperforms the persistence method.

However, there are some drawbacks when using lidar data for forecasting. One of the major barriers to overcome is the availability of the measurements. The lidar measurement principle is based on the interaction of laser pulses with particles suspended in the air. The wavelength of the backscattered light is shifted relative to the speed of the aerosols according to the Doppler principle [41]. This means that the measurement depends on the existence of these aerosols and if the concentration in the air is too high or too low, the device records a noisy signal. It also means that the measurement range fluctuates due to environmental conditions such as fog or rain showers [38]. And as the measurement range determines the forecast horizon, realtime forecasts are not possible if the lidar is blind. As physics cannot be changed, and the measurement principle is what it is, as a consequence a fallback solution needs to be implemented in case the lidar does not provide measurements. Data from other sensors such as radar or drone measurements could be one solution. Using statistical models (see Section 5.2.1) or the coupling of the measurements with NWP models (cf. Section 5.2.2) could be another solution. Also more investigations have to be carried out to determine the optimum conditions for good range measurements of lidars.

Another drawback of lidars so far have been the high costs and the inaccuracies of signals in complex terrain. According to the white paper of the Deutsche Windguard [42] and [43], especially “in complex terrain sites, influence of the relatively large scanning volume of today’s LiDAR and SODAR must be carefully considered in terms of its influence on the measurement accuracy...”. This has been a general observation and an ongoing research topic [see e.g., 44–49]. A solution provides the measurement with multiple, synchronised scanning lidars that enable the direct measurements of wind field components [see e.g., 50,51].

Another obstacle when working with lidars is that currently there is no standard or Recommended Practices for the use of scanning lidar for wind speed forecasting. More research is needed to find out what the ideal measurement setup looks like, in particular how many lidars are needed and where to place those devices within a wind farm. Also the optimal measurement strategy is not clear. To that end different use cases have to be investigated to find out what the best campaign setup and measurement strategy is. Such use cases should include on- and offshore wind farms of different scales. Recommended practices then need to be consolidated so that the widespread use of lidar for forecasting becomes possible on a commercial level.

5.1.2. Radar-based forecasts

Radar are remote sensing systems which can determine the position, angle or motion of objects and are being used in multiple applications including traffic control, ocean surveillance, weather monitoring, flight control systems and antimissile systems. Similar to wind lidars, Doppler radars can be used for wind power forecasting as they are able to determine the velocity of the objects. The

417 working principle is the same as for lidars, but rather than sending light waves, they emit radio waves.
418 Thus, in an environment where meteorological particles with high humidity such as water droplets or
419 ice crystals are present, radars are able to measure the wind speed by determining the motion of the
420 hit particles.

421 The maximum range that radars can measure is given by the wavelength of the signal emitted, but
422 in this paper we only focus on radars which work on wavelengths that are of interest for minute-scale
423 forecasting of wind power. Thus, we limit our review to radars working between the C-Band and the
424 Ka-band radars, or with a wavelength of 3.2 cm to 8.6 mm.

425 Doppler-radars working in the Ka-band (35 GHz) are optimal candidates for wind power
426 forecasting (Figure 6). The short wavelength employed allows for high temporal and spatial resolution
427 of the measured wind fields. As lidars, Doppler radars measure the LOS wind speed. Thus, measuring
428 with one Doppler radar over a defined Plan Position Indicator (PPI) trajectory, the horizontal wind
429 speed can be determined by applying a VAD retrieval technique. To derive the two horizontal wind
430 speed components, two synchronized Doppler radars are needed [52]. The number of publications
431 on the use of Doppler radars for wind energy applications has grown in the last years. Hirth et al.
432 coupled wind farm operational data with wind fields measured by two synchronized Doppler radars
433 (dual-Doppler radar) to further investigate wind farm wake effects [53]. Dual-Doppler measurements
434 of the wake behind an offshore wind farm were also reported by Nygaard et al. [54]. The performance
435 of wind turbines was also validated with dual-Doppler measurements in [55].

436 First evidence of the promising application of Doppler radar systems for forecasting purposes was
437 documented by Hirth et al. [56]. An extreme wind ramp event observed by the Texas Tech University
438 Ka-band radars at a wind farm in Oklahoma was presented. The authors merged dual-Doppler wind
439 fields with operational data from 32 wind turbines to document the observed transient wind event
440 and its effect on the wind turbines' performance. They also coupled data from a meteorological tower
441 to analyze the weather conditions that originated the transient event.

442 Recently, it was shown that Doppler radar observations can be employed to derive minute-scale
443 density forecasts of wind power. In [57] the authors proposed a methodology that uses dual-Doppler
444 radar observations of wind speed and direction in front of a wind turbine to forecast the power
445 generated in a probabilistic framework. In a case study, they predicted the power generated by seven
446 turbines "free-wake" wind turbines in an offshore wind farm. Predictions were generated with a
447 temporal resolution of one minute and with a lead time of five minutes. With their study, the authors
448 showed that the radar-based forecasting model is able to outperform the persistence and climatology
449 benchmarks in terms of overall forecasting skill and generate reliable density forecasts in the case of
450 optimized trajectories.

451 One of the main advantages of Doppler radars is the extended range they can measure (over
452 30 km). Additionally, the optimal trade-off between the temporal (one minute) and spatial (50 m)
453 resolution of dual-Doppler radar measurements, compared to that of typical wind measurements from
454 met-masts or satellites, makes them promising candidates for minute-scale forecasting of wind power.
455 As with lidars, the same wind power forecasting process can be implemented to derive a wind power
456 forecast. Besides, the fact that they can perform volumetric measurements (wind field measurements
457 at multiple heights), allows to infer further information such as horizontal and vertical wind shear.

458 However, as with lidars, one of the main obstacles to the adoption of radar as a forecasting tool
459 is the availability of the measurements. The radar measurement principle lies in the backscattering
460 of particles in the air containing high humidity such as water droplets or ice crystals. Therefore, the
461 quality of the measurements relies on the concentration of these particles in the air [52]. Besides, the
462 relatively large dimensions of Doppler radars complicate their installation and reduces the range of
463 possibilities for placing them, especially in offshore environments. The advantage of Doppler radar
464 with respect to lidars is the maximum range that they can measure. However, compared to lidars, the
465 wider beam width of radar results in larger beam spread at large ranges.



Figure 6. One of the two Doppler radar units deployed for the BEACon project [54,57].

466 Although we have mainly focused on the use of Doppler radars for forecasting applications,
467 weather radars have been also identified as promising candidates for very short-term power forecasting
468 of offshore wind power. Modern weather radars working in the C and X-band measure the intensity
469 of precipitation. They are, consequently, able to anticipate precipitation fields associated with severe
470 wind speed and power fluctuations. The capabilities of anticipating strong wind power fluctuations in
471 offshore wind farms using local weather radars was introduced in [58]. In their work the authors were
472 able to track the arrival of precipitation events to the surroundings of an offshore wind farm. These
473 events were highly correlated with the strong observed power fluctuations. The authors also identified
474 shortcomings of the use of weather radars for wind power forecasting, which included: interception of
475 radar waves (cluttering), beam attenuation due to intense precipitation, anomalous propagation of
476 the radar waves during specific atmospheric conditions, underestimation of precipitation reflectivity
477 (bean filling) during convective events, and overshooting at long ranges due to the curvature of the
478 Earth.

479 5.1.3. Lessons learned with remote sensing instruments in real-time forecasting projects

480 Several research projects have been conducted with the goal of integrating remote sensing
481 measurement into real-time forecasting projects. For this purpose not only scanning devices were
482 deployed, but also profiling, ground-based devices. In the largest and longest measurement campaigns
483 targeted towards real-time forecasting of wind energy in recent years were two projects funded by the
484 United States Department of Energy, the wind forecasting improvement project (WFIP I and II) [59]
485 there were used 12 wind profiling radars, 13 sodars and three lidars amongst other meteorological
486 sensors. The lidars as well as sodars are basic equipment used in meteorological data assimilation
487 today and have been quality checked following meteorological standards through the Meteorological
488 Assimilation Data Ingest System (MADIS) [60]. This was a necessary step in order to improve the
489 simulation into the real-time model forecast systems [61]. In the second project, “Distributed Resource
490 Energy Analysis and Management System (DREAMS) Development for Real-time Grid”, a number
491 of sodars, lidars were used to enhance the Hawaiian system operator’s EMS (Energy Management
492 System) tools for situational awareness in critical events [62]. Here, the instruments were for the first
493 time part of the operational management system at a system operator in real-time.

494 From the above described studies and experimental measuring campaigns as well as real-time
495 testing it can be concluded that the remote sensing instruments need to be serviced well and maintained
496 similarly to any other real-time instrument operating under changing conditions throughout the yearly
497 cycles. If this is not done, echoes, interfering noise sources, laser beam disturbances deteriorate
498 the instruments and make the further processing of the data impossible and the quality of the data
499 deteriorates significantly over time. It is also commonly understood that it requires skilled personnel
500 to install and maintain such instrumentation, if it should run continuously and reliably.

501 The following lists their findings and recommended technical requirements to ensure high quality
502 data in long-term real-time operation:

- 503 • Lightning protection and recovery strategy after lightning should be ensured.
- 504 • Instruments must be serviced and maintained by skilled staff.
- 505 • Version control must be maintained for signal processing.
- 506 • Measurements must be raw or technical requirements must include maintenance and software
507 updates.
- 508 • Wind characteristics data should be measured at a height appropriate for the wind farm, either at
hub height or preferable at both hub height and the lowest possible measuring height (e.g. 30 m).
- 509 • Remote sensing devices in complex terrain require special consideration.

511 From these findings and studied projects and measurement campaigns, it can be concluded that in
512 active weather conditions, i.e. at the flat range of the power curve as well as under strong precipitation
513 events, it must be expected that met mast anemometers are more reliable than sodar or lidar devices.
514 From a forecasting and operational monitoring perspective, it has been found that the conditions
515 outside of the instrument's range are some of the most critical conditions for grid operation, such as
516 storms with precipitation or high winds. Sodars are more prone to data delivery failures than lidar,
517 but to this date it is still also an issue for lidar devices that measurement information is not accessible
518 in critical conditions, where it is most needed.

519 5.2. Adaptation of models with different types of measurements

520 When there is sparse, inaccurate, irregularly distributed data in space and time which is generally
521 the case in atmospheric science, models can be used to infer the evolving state of the system. However,
522 to infer the evolving state of the system being modeled, data needs to be employed or assimilated by a
523 model. This model can employ physical single point or multiple point time series data that calibrates
524 itself based on measurements or spatially distributed time dependent or independent physical model
525 that assimilates which will be discussed in the next sections.

526 5.2.1. Statistical time series models

527 Statistical approaches to forecasting problems mainly rely on deducing patterns from past
528 observational data and extrapolating these relationships to predict future values over a desired
529 time step. With wind energy applications in mind, in this section we consider the task of forecasting
530 a one dimensional time series signal such as a wind speed measurement, or a SCADA source such
531 as wind turbine or wind farm active power signal. The chosen forecast horizon should relate to
532 the time resolution of available input data, and at minimum be one sample (time step) ahead to
533 avoid errors introduced by interpolation. Statistical forecasting methods used on the minute scale are
534 largely identical to techniques employed for longer horizons. The main differences being the temporal
535 resolution of the data and the variability of the physical process being predicted (see Section 2).

536 Data acquisition systems are ordinarily capable of sampling and saving data at high frequency,
537 although historically this data has not always been used nor recorded. For the purposes of minute-scale
538 forecasting, 10-minute or hourly averaged data sets are not sufficient for capturing signal characteristics
539 needed to construct and validate a well performing statistical model. For this reason we recommend
540 that all data generators ensure that they have access to and are logging their high frequency data (both

turbine and meteorological sources), and that the instruments are properly maintained. The lower bound of the recorded sampling rate should be at minimum twice the highest frequency in the analog signal you wish to capture, in order to avoid aliasing in the discrete signal transformation (Nyquist sampling theorem). In practice, 1 Hz (1 sample per second) is proposed as a compromise between functionality and transmission/storage considerations. This will allow for future model building and testing which can resolve fluctuations on the minute-scale.

Time series data contrasts to cross-sectional data in that it is naturally ordered in time. Samples which are closer together will normally express a higher correlation than those further apart. This temporal link should be explored through inspection of the autocorrelation and partial autocorrelation function of the time series before beginning any attempts to build a model.

There are often a number of characteristic sub-components embedded in the time series which can be obtained through decomposition techniques in order to normalise samples across time. Examples include differencing an integrated series, removing an overall trend (usually by either mean subtraction or model fitting to obtain the residuals), accounting for cyclic fluctuations, and adjusting for seasonal variations.

A common assumption made by statistical forecasting methods is that of stationarity. Stationary processes comprise of data where the mean, variance, and autocorrelation structure do not change over time. By implementing the techniques described above, it is possible to transform a non-stationary time series into a stationary one which can be used with traditional forecasting methods.

Benchmarking in any forecasting exercise is crucial. Commonly for forecasting at these short timescales the persistence and climatology models are employed; these simple methods assume that the forecast for the target variable is the most recent available measurement or summary statistics of historical measurements, respectively. Statistical methods for wind speed and power forecasting are typically based on time-series models such as autoregressive [63] (AR) and autoregressive moving average (ARMA) [64,65] models as well as other soft computing techniques such as neural networks [66].

Purely AR models are formulated as a weighted combination of past observations (lags) where the coefficients are normally estimated via ordinary least squares regression. The order of the AR model, or maximum lag, is crucial and can be chosen most simply by inspection of the auto-correlation and partial auto-correlation functions of the signal. Cross-validation or an information criterion provide an alternative method for defining the model order. Domain knowledge of the local meteorological conditions can also be used to extend these simple models. For example, in certain regions the wind/power time series may exhibit strong diurnal trends which would necessitate the inclusion of time-of-day into the model.

Beyond time series models, machine learning techniques also are widely employed. These techniques can be more flexible than classic time series models in terms of easily allowing for more explanatory variables and are typically more naturally able to capture non-linear relationships. It should be noted that this comes at the expense of additional model tuning to optimize algorithm specific hyper-parameters and possible overfitting of the data unless careful cross-validation procedures are followed. Examples include artificial neural networks [66], hybrid multi-models with blending [67] together with feature selection [68], and penalized regression [69].

Artificial neural networks, particularly recurrent neural networks (RNN), have been widely applied for sequence prediction including time-series data. Long short-term memory (LSTM) networks are explicitly designed to capture data patterns of arbitrary lags, and assimilate long-term temporal dependencies [70]. This has led to numerous applications in energy forecasting which outperform traditional time-series modelling approaches. Wu et al. [71] demonstrates such a probabilistic 4-hour ahead wind power forecast model employing a LSTM network architecture.

Statistical forecasting models can also be made dependent on the current behaviour of the target time-series or on exogenous variable(s). These are termed regime-switching models and can be based on unobserved regimes [72,73] or by observed regimes like atmospheric conditions [74,75]. It follows

591 that these regimes can be derived from lidar/radar measurements [76]. The benefit of regime switching
592 is that the statistical models can react faster to changing conditions, as opposed to having a fixed
593 coefficient models or by tracking slower changes in behaviour via for instance an online update of the
594 coefficient estimates.

595 Concurrent information from spatially distributed wind farm or met mast measurements also
596 provide a route for improvements in forecast skill [77,77]. Multivariate forecasts which encode
597 information on the spatio-temporal dependency of neighbouring sites can be tackled via a vector
598 autoregressive models (VAR) at these time horizons. With an increasing number of sites, making
599 sparse estimates of the coefficient matrices becomes more important, as does estimating them via
600 efficient numerical procedures [78–80].

601 Forecast uncertainty at these horizons can also be accounted for via probabilistic density forecasts,
602 quantiles, or prediction intervals [81]. These may be generated using parametric assumptions of the
603 forecast distribution shape [63] [82] or non-parametric techniques [83] [84]. Uncertainty forecasts
604 enable the user to manage risk in decision making and leverage more actionable information from
605 their data, if information content is communicated properly [85].

606 These discussed statistical methods have been widely proven to increase forecast skill over
607 persistence at time-horizons generally at a minimum of 10 minutes ahead. Further research is required
608 to evaluate the suitability of statistical methods below this time horizon and at what time range
609 forward facing lidar/radar based systems or hybrid statistical and radar/lidar systems are a more
610 suitable choice.

611 5.2.2. Statistical data assimilation based on physical models

612 Data assimilation performs an essential role in the forecasts of wind power systems. While the
613 concept is very inclusive, meaning inherently assimilation of any data with any model, in this section,
614 the term is used in more exclusive sense without addressing statistical time series models, which is a
615 special case of data assimilation where usually non-physical models are taken into consideration. This
616 was discussed in the previous section. The concept is inherent from the fact that neither the model nor
617 the observations are perfect. As a result to have an accurate state of the system, the numerical model
618 without guidance of how accurate the current state is, is not sufficient and guidance from observations
619 is required. This is even more so for weather forecast systems, where the system itself is very sensitive
620 to initial conditions and boundary conditions. Data assimilation was employed first in engineering
621 however it is more than an engineering tool today.

622 In summary, data assimilation is the technique to adopt multiple measurements and observations
623 of different types into a 3-dimensional model space. In meteorology it is used to generate an initial
624 state of the atmosphere from observations that is required as input field, together with boundary
625 conditions to any numerical weather prediction (NWP) model.

626 In renewable energy production, data assimilation and state estimation also has an important
627 role, in a classical way, but also with possibility of assimilation on control zone level or even park level.
628 System operators and Wind farm operators require advanced knowledge of ramp-up and ramp-down
629 events [86–88]. In a ramp/extreme event forecast you want to analyze and use outliers in order to get
630 the risk of a critical ramp/event to occur, while some data assimilation algorithms can dismiss outliers.
631 The increased frequency of assimilation can address this challenge. The frequency of assimilation
632 is important for ramp prediction, while the challenge comes from the model size and assimilation
633 method chosen for the task, however simplified models with higher frequency can be adapted for the
634 applications discussed here.

635 The work on data assimilation and state estimation spans many disciplines and several
636 decades, where various approaches of data assimilation to adapt numerical weather model states to
637 measurements [89,90] have been developed. The initial development of data assimilation has started
638 as an objective analysis [e.g., 91,92], which was also referred as successive correction methods.

639 This work was followed by optimum interpolation (OI) [e.g. 89,93]. In the sequential data
640 assimilation techniques, the model solution is recursively updated during a forward integration with
641 weights on observations and model output according to their corresponding uncertainties. These
642 uncertainties are static and based on predefined model output statistics and hence lack the dynamical
643 and non-linear behaviour of the weather and model system. OI methods have lead to development
644 of variational methods in data assimilation, where constraints were introduced in variational data
645 assimilation methods. These methods are namely 1DVAR, 2DVAR, 3DVAR [e.g. 94,95] and 4DVAR
646 [96,97, e.g.,] where D stands for Dimension. Variational approaches can be also formulated in the
647 context of a Bayesian problem.

648 In parallel the Kalman filter was introduced which is an observer feedback control system. The
649 main difference between 4DVar and Kalman filters are the way that they address the mode and mean
650 when the distributions are non-normal. There are several existing methods used in state estimation and
651 data assimilation and most of them are based on the Kalman filtering theory introduced by Kalman
652 and Bucy [98]. The pure form of the Kalman filter has been widely employed for the state estimation
653 of the linear Gaussian systems [99], however it is linear and is not preferred for non-Gaussian and
654 nonlinear systems [99,100]. For transition of Kalman filtering to the nonlinear and non-Gaussian
655 systems, techniques such as extended Kalman filter (EKF), ensemble Kalman filter (EnKF), unscented
656 Kalman filter (UKF) and particle filter (PF) algorithms are developed [99,100] and are employed to
657 wide range of problems from low to high dimensional systems. The EKF method is implemented by
658 linearisation of the non-linearities via using a Jacobian matrix. The EnKF uses Monte Carlo methods
659 that helps to estimate the error covariances of the background error, gets an approximation to the
660 Kalman-Bucy filter and produces an ensemble of initial conditions that can be utilized in an ensemble
661 forecasting system. The EnKF embeds the non-linearities into the original linear KF solution and it
662 uses an extra covariance inflation to consider the nonlinearities [101,102]. Later, adjustment solutions
663 [e.g., 103] and also sequential solutions of the filter have been developed [e.g., 104].

664 Some of the limitation of the Kalman filter technique in meteorological context is however not a
665 limitation in wind power context, because there the area of observational distribution is rather small,
666 even if the area spans over an entire country. Most of the data used in meteorology are sparse in
667 time, but widespread over the entire globe. Nevertheless, if the traditional KF should be applied
668 for a data assimilation task in a wind power context, where the true state of the atmosphere is the
669 target, this would imply that the models would have to generate forecasts in a small area, which is
670 undesired, or it would require unrealistically many computing resources and observational input
671 of meteorological variables. As described by Anderson and Anderson [103] and Houtekamer and
672 Mitchell [104], the standard KF propagates the error covariance from one assimilation step to the
673 next, which is computationally expensive. In the EnKF, this procedure is approximated by using an
674 ensemble of short-range forecasts, where the forecast error covariance is directly computed from the
675 ensemble when they are needed for the data assimilation. Meng and Zhang [105] found that it was
676 beneficial to use a multi-scheme ensemble approach rather than a single-scheme approach, because it
677 does not require such a large ensemble size to cover the uncertainties. They built an ensemble based
678 on a Penn-State University WRF model kernel and different parameterisation schemes. Möhrlein et al.
679 [106] developed what they called an “inverted” Kalman Filter approach where they make use of the
680 ensemble Kalman filter technique and translate this into a wind power context. This approach does
681 not only solve the problem of distribution of observations in space, but also in time. By taking the
682 weather situation into account, the well-known timing problem (phase errors) and temporal influence
683 of measurements can be solved mathematically with the help of a forecast covariance matrix. The
684 additional feature of making use of situations with anti-correlating weather conditions adds to the
685 physical correctness of the approach, as it identifies, where the borders, or in meteorological context,
686 fronts are in space and time.

687 This feature is an important factor, especially, if large wind farms are located in a relatively small
688 area, where sharp fronts pass over the area and where there is risk for cut-off or situations of rapid

decrease of power production over short times. Such situations are for example reported regularly at offshore wind farms in the North Sea, Baltic Sea, the United Kingdom, Ireland, Alberta, Canada and Oregon, USA at the foothills of the Rocky Mountains.

Möhrlen et al. [106] set up an inverted Ensemble Kalman Filter approach (iEnKF) that is designed for short-term wind and solar energy forecasting, upscaling and data assimilation. They report that this type of iEnKF approach has been tested in a number of areas around the world and its capabilities demonstrated with large amount of measurements, typical for a TSO area with larger amounts of wind and solar power on the grid. The algorithm allows for any kind of measurements that is in any kind of relation to the target parameter, e.g. wind power, solar power to be used and mixed into the matrices. Hence, it is the first physically consistent methodology, where meteorological ensemble forecasts provide the framework for the distribution of observational influence and where it is possible to back-scale aggregated total production measures of an area physically consistent for the statistical training of wind power forecasts (see Figure 7). In that sense the iEnKF provides an indirect feedback mechanism to the NWP input for the generation of power curves.

This is a milestone in variable energy generation forecasting and is of great value for the large-scale integration and requirements of reliable handling of these power sources for transmission system operators, and also for traders and wind farm operators in the electricity markets with fast growing wind capacity and liberalised market rules, especially because it can be applied on all time scales, from minutes to hours ahead, as it has an inherent dependency of the measurement influence on the forecasts built into it. The computationally expensive part of this point assimilation technique is done on the typical 6-hourly meteorological cycle, while the Kalman Filter can run on minute basis handling thousands of measurements within a few seconds due to the simple linear algebra that the covariance matrix computations are based on.

The unscented Kalman filter (UKF) employs the calculation of an approximate mean and covariance as a linear combination of a number of propagated points (called as sigma points). The PF and its variants also use the Monte Carlo simulation with sampling method based approximation of the posterior density of the state vector rather than doing any explicit functions so it simulates non-linearity and non-Gaussianity. Even though PF is a competent tool for the estimation of the nonlinear and non-Gaussian systems [107], it can be computationally demanding because of size that increases accuracy however this can be addressed adaptively with careful selection of ensembles introduced by Uzunoğlu [108].

The computational complexity in the above summarized methods can be addressed in the subspace of ensembles that was one of the focuses of the Maximum Likelihood Ensemble Filter (MLEF) that employs ensembles in the pre-conditioner. This approach differs from the EnKF and PF by working on state space rather than sample space and it optimizes a nonlinear cost function through maximum likelihood practice which reduces the computational time and addresses the stochasticity and the discontinuity while it utilizes the sampling in low dimensional space and employs the Hessian information. This method has been applied to many disciplines such as power systems as well as to the wind energy industry [19,109]. In the workshop, the successful application of this method to second scales were presented.

5.2.3. Use of different types of measurements to identify extreme events

Extreme events in a meteorological sense are events that deviate from the mean and exceed beyond specific threshold values. In the power system, extreme events can occur under meteorological average conditions as well and not be considered extreme, when meteorological threshold values, such as wind speed, are exceeded. The differences are mainly due to the constraints in the power lines and the supply and demand relationship. Only in areas where wind turbines shut down due to high wind speeds - so called high-speed shutdowns can such wind speeds challenge both life and the ability to safely control the grid.

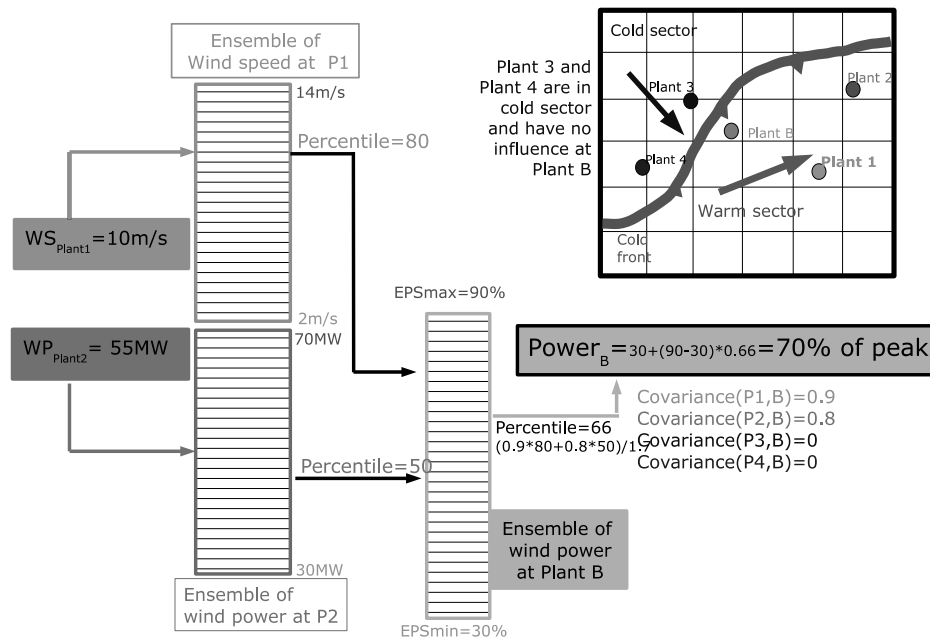


Figure 7. Functionality of the inverted Ensemble Kalman Filter when using different kind of measurements.

737 The way to deal with extreme events in both meteorology and the power industry is by applying
 738 uncertainty forecasts that provide an objective measure of the possible extreme. Deterministic forecasts
 739 cannot serve such situations, as they are tuned for best average conditions, i.e. in the setup, statistical
 740 training and model output statistics, outliers and extremes are filtered out. While statistical approaches
 741 can be used in many life science applications, in power system applications, it is crucial to employ
 742 an approach that provides a valid uncertainty of the forecast inclusive extremes in every hour of
 743 the forecast. Such extreme forecasts must be established based on probabilities computed from a
 744 probabilistic prediction system that can take the spatial and temporal scales into consideration in order
 745 to capture the temporal evolution and spatial scale of e.g. low pressure systems that contain wind
 746 speeds leading to large scale shut-down of wind farms.

747 This can for example be provided by such a physical approach based on a NWP ensemble that
 748 ideally contains all extreme values inherent in the approach without the requirement of statistical
 749 training such as the multi-scheme method. Alternative solutions may exist from statistical approaches
 750 by employing an extreme event analysis to a statistical ensemble [see e.g., 85]. However, statistical
 751 approaches are always limited to past climatology and require large amounts of data. The requirement
 752 for such forecasts is that they must be able to provide probabilities of extreme events, where each
 753 forecast or “forecast member” provides a valid and consistent scenario of the event. The probabilities
 754 need to be suitable solutions for a decision process. They can be computed for very critical and less
 755 critical events, depending on the end-users’ requirements.

756 If the target is to achieve a feedback mechanism for all kinds of data that are in any kind of
 757 relation to wind or solar power data, which by default is not reversible, the solution requires a unified
 758 methodology to measure the value of an observation and its impact on the total system. This is a
 759 well known problem in meteorology, which has been extensively researched, because more and more
 760 sophisticated observational instrumentation is developed and deployed that require transformations
 761 of observations into the numerical weather prediction systems [105,110–113].

762 Modern Doppler radar measurements for example require retrieval transformation algorithms,
763 where wind fields are computed with continuity equations and the thermodynamic properties through
764 physical constraints, once the wind field is known. Snyder and Zhang [112] and Zhang et al. [113]
765 discovered that the ensemble Kalman filter is a practical approach for the generation of state estimates
766 with convective-scale data assimilation from such Doppler radar measurements. Applying an EnKF
767 approach [28] with input from a multi-scheme ensemble is able to use an inherent intelligence, if the
768 input ensemble data contains a combination of historical calibration, actual and historic weather and a
769 transformation method for the use of different types of measurements. Generating percentiles from
770 such an ensemble method enables the construction of a uniform covariance matrix and in fact ensures
771 that measurements are handled consistently without the need of any physical considerations of their
772 compatibility or irreversibility inside the iEnKF itself. The example in Figure 7 shows the functionality
773 of an inverted Kalman Filter approach for the assimilation of point measurements in (wind and solar)
774 power space with a multi-scheme ensemble approach. This MSEPS (multi-scheme ensemble prediction
775 system) has 75 ensemble members with various different parameterisation schemes for the advection
776 and the fast physical processes such as condensation and vertical diffusion. The principles of this
777 MSEPS are described in detail in [106]. The spread in the MSEPS is physically based, because all
778 members in the ensemble are essentially equally valid descriptions of the physical properties in the
779 atmosphere and full-scale NWP models. The iEnKF method in combination with ensemble forecasts
780 follows in principle these developments in data assimilation methodologies and hence provides a
781 compatible and extendible solution with the combination of meteorological and wind and solar power
782 observations and also presents major improvements and reliability enhancement in the short-term
783 forecasting and data assimilation of wind and solar power.

784 *5.3. Overview of methods for minute-scale forecasting*

785 Table 2 provides an overview and summary of the different minute-scale prediction methods,
786 their forecasting horizons as well as advantages and barriers to the adoption of the methods. It also
787 lists solutions that are suggested as a way forward to overcome the barriers.

Table 2. Overview of methods for minute-scale forecasting

Method	Input Data	Forecast Horizon	Advantage	Barrier	Solution	References
Scanning lidar-based forecast	Lidar data	30 min	<ul style="list-style-type: none"> – The measurements provide comprehensive knowledge of the wind field several kilometres upstream of a wind turbine or wind farm. – The possibility of scanning vertical wind profiles are important information on power production of turbines (e.g. detection of low level jets) – Modern lidars are compact in size and allow for flexible measurement campaigns, they are cheaper than met masts. 	<ul style="list-style-type: none"> – The measurement range and thus the forecast horizon of the lidar fluctuates due to environmental conditions. – It is not clear yet what the ideal measurement setup for forecasting is and there is no standard available. – Data signals are software dependent, which can be challenging in a real-time environment, where data cannot be modified with post-processing 	<ul style="list-style-type: none"> – In case the lidar does not provide data, there is a need for a fallback method that is sufficiently good on its own, eg. NWP model where the data is assimilated. – Different use cases of using lidars for forecasting have to be investigated to find out what the best campaign setup is. Standards can then be deduced. – Regular service and calibration reduces the risk of faulty signal processing, but increases costs. 	[34,37–39]

788 6. Challenges for the implementation of minute-scale forecasting in large energy systems

789 There are several use cases for predictions shorter than 1 to 2 hours. In Australia, the system runs
790 on a 5-min schedule [114] and requires renewable energy and load forecasts on those time scales. In
791 Germany, renewable energy plants can be pre-qualified to participate in the reserve market, and need
792 to predict their possible power with less than 5% accuracy in the pilot phase and less than 3.3% in
793 the implementation phase. This is calculated in one-minute intervals. In Denmark, with hourly wind
794 penetrations of over 140%, the grid is run proactively in hourly steps, predicting the imbalance and
795 reacting accordingly on the basis of spatio-temporal forecasts [115]. So the use cases for minute scale
796 forecasts are there, and the best forecasts require upstream information in real time.

797 In a large energy system with moderate penetration from wind sources, a system operator can
798 choose to outsource balancing of wind. This is the approach chosen widely in central Europe. A major
799 reason behind the liberalized strategy in Europe is a wish to make the market more competitive and
800 indeed it happened faster than anybody expected in both Denmark (2009) and Germany (2012) [116]
801 with the result of lower spot market prices in the NordPool market and the German-Austrian part of
802 EPEX.

803 The difference between a TSO and a power trader's prioritized optimization lies in the target
804 horizon. The trader is looking up to several weeks ahead, while the TSO's optimisation horizon is
805 over one year. In particular once the commercial path is taken, then the TSO lacks information about
806 the generation and must rely on the information from the trading companies. In Germany, the TSOs
807 have today little control of the renewable energy generation and relies on out-sourced solutions for
808 critical system information to a degree, which has not been considered acceptable for many years from
809 a system security perspective.

810 Although Germany has the highest capacity of wind and solar generation in Europe, it is apparent
811 that the system lacks information for optimization. This is seen in frequent down regulation of wind
812 farms in day-time and recovery during the middle of the night, often many hours after the wind
813 has dropped again. This process has become highly inefficient in recent years, because there are no
814 requirements for wind farms to provide real-time data to the system operator.

815 German experience shows that wind energy loses efficiency and value unless there are obligations
816 for wind farms to provide data required by various forecasting and system operation processes.

817 Based on this experience, it is crucial to define standards regarding setup and maintenance of
818 instrumentation, collection and provision of data, as well as required quality of data. Beside the
819 standards, in transparent markets the grid codes should also contain a clear definition about the rights
820 on the use and the obligation to provide the data. Without such regulations, the required quality is
821 hard to achieve in order to improve forecasts. Corrupt and wrongly calibrated instrumentation can do
822 more damage to a forecast than not having data. This is one of the greatest challenges at present and
823 the reason for slow progress on minute-scale forecasting. Especially in large systems such as Germany
824 with many thousands of individual wind turbines and small wind farms, this is a difficult challenge to
825 overcome. Nevertheless, the need to make appropriate changes to the grid codes is the same for all
826 markets.

827 7. Conclusions

828 Minute-scale forecasting of wind power is a discipline that is becoming crucial to accomplish in
829 globally transitioning power systems with increasing amounts of variable generating power sources
830 from renewables. The participants of the collaborative IEA Wind Task 32 and 36 workshop established
831 a framework for forecasting at the minute scale and discussed new techniques that will push the limits
832 of state-of-the-art forecasting methods to a new level.

833 Three applications were identified that can benefit from minute-scale forecasting and their
834 respective forecasting horizons. Wind turbine and wind farm controllers need wind speed forecasts
835 to optimize the turbine and farm operation. The task of balancing the power grid and optimizing
836 energy markets relies heavily on precise wind power forecasts as well. To carry out forecasts that range

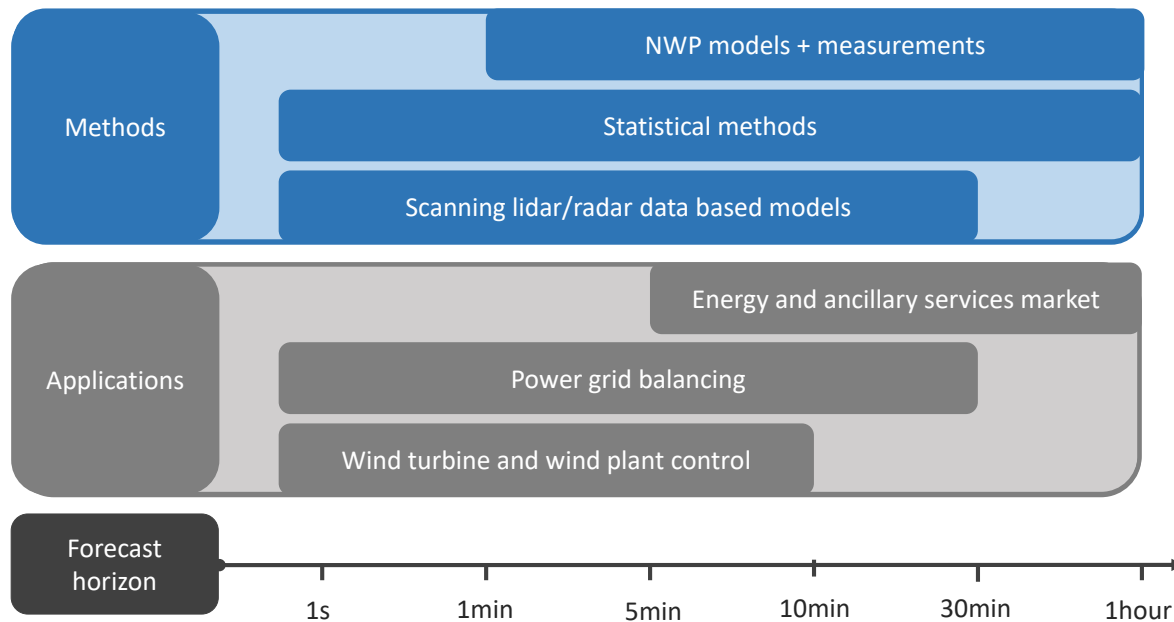


Figure 8. Overview of forecast horizons of different wind energy applications and forecast methods in the second and minute scale.

from 1 second to 60 minutes, forecasters have the choice between different methods (Figure 8). In our discussions at the workshop and this review we differentiate between using preview data from remote sensing devices, statistical approaches that deduce patterns from observational data to predict future values and finally methods that are based on data assimilation into physical models. These assimilated data can originate both from remote sensing devices or other existing observational data sources from meteorological masts or wind turbine data.

By investigating more deeply the respective methods it became clear that they all have advantages, but also barriers that need to be overcome in order to achieve reliable forecasts on a commercial level. The following list provides an overview of focus areas for the near future to advance further with minute-scale forecasting:

- **Research requirements.** At this point, many methods are still under development. There are a lot of open questions to solve and the optimal forecasting techniques for the different applications has not been found yet. It is also not sufficiently demonstrated that all methods add value. So more research needs to be carried out and both measurement experts and meteorological modelers need to collaborate closely to find solutions.
- **Data requirements.** All forecasting methods rely on data. This might sound obvious, but what is needed is high resolution, high quality data delivered in real-time to forecast systems. Wind turbine or wind farm operators often only log 10-minute averages of their operational data. However, to train and validate models, high frequency data is necessary.
- **Requirement for standards.** End users have more confidence in data when the collection and use of the data is supported by recommended practices and standards. Community-driven recommended practices are available for some applications of wind lidar but not in the context of forecasting.
- **Expert training.** As with any emerging technology, there are a limited number of experts that know how to carry out a remote sensing measurement campaign, feed data into neural networks or are capable of assimilating data into a NWP model. This forms a barrier to the widespread commercialization of minutes-scale forecasting. IEA Wind Tasks provide an ideal platform for

the international exchange and dissemination of knowledge order to establish more widespread training in this topic.

Supplementary Materials: IEA Wind Task 32 is operated by the Chair of Wind Energy at the Institute of Aircraft Design at the Faculty of Aerospace Engineering at the University of Stuttgart. More details about IEA Wind Task 32, including minutes from the workshops and other documents, can be found at www.ieawindtask32.org. IEA Wind Task 36 Forecasting is operated by Gregor Giebel of DTU Wind Energy at Risø, Denmark. See www.ieawindforecasting.dk for more information. General information about IEA Wind can be found at www.ieawind.org. IEA Wind TCP functions within a framework created by the International Energy Agency. Views, findings, and publications of the IEA Wind TCP do not necessarily represent the views or policies of the IEA Secretariat or of all its individual member countries. IEA Wind TCP is part of IEA's Technology Collaboration Programme (TCP).

Author Contributions: Ines Würth was a co-organizer of the workshop, led the paper and wrote the abstract, introduction, Section 5.1.1, conclusion, some section introductions, and edited all sections. Laura Valldecabres Sanmartin was a co-organizer of the workshop, was a co-editor of this paper, led Section 2, 3.3 and 5.1.2 and contributed to Section 5.1.1, and 5.1. Elliot Simon was a co-organizer of the workshop, led Section 5.2.1, and contributed text in Sections: 2, 5.1.1, and 5.1. David Schlipf led Section 3.1. Bahri Uzunoğlu led Section 3.2 and wrote Section 5.2.2 and 5.2.3 together with Corinna Mörlen who also led Section 4 and 5.1.3 and contributed to Section 5.1, 5.2.1, 3.3 and 6. Gregor Giebel contributed to Section 4. Ciaran Gilbert contributed to Section 5.2.1. Anton Kaifel and all other co-authors participated in the paper review and revision process.

Funding: This publication was supported by the Open Access Publishing Fund of the University of Stuttgart and has received funding from the European Union's Horizon 2020 research and innovation programme under the Marie Skłodowska-Curie Grant No. 642108.

Acknowledgments: We would like to thank DTU Wind Energy (Risø campus) for graciously hosting the workshop, and all of the workshop participants who contributed their ideas and knowledge.

Conflicts of Interest: The authors declare no conflict of interest.

References

1. Giebel, G.; Brownsword, R.; Kariniotakis, G.; Denhard, M.; Draxl, C. The State-Of-The-Art in Short-Term Prediction of Wind Power. Technical report, Technical University of Denmark (DTU), Roskilde, Denmark, 2011. doi:10.11581/DTU:00000017.
2. Fraile, D.; Mbistrova, A. Wind in power 2017: Annual combined onshore and offshore wind energy statistics. Technical report, WindEurope, 2018.
3. Fraile, D.; Komusanac, I. Wind energy in Europe: Outlook to 2022. Technical report, WindEurope, 2018.
4. Larsén, X.; Larsen, S.; Lundtang Petersen, E. Full-Scale Spectrum of Boundary-Layer Winds. *Boundary-Layer Meteorology* **2016**, *159*, 349–371. doi:10.1007/s10546-016-0129-x.
5. Apt, J. The spectrum of power from wind turbines. *Journal of Power Sources* **2007**, *169*, 369–374. doi:10.1016/j.jpowsour.2007.02.077.
6. Vincent, C.L.; Trombe, P.J. 8 - Forecasting intrahourly variability of wind generation. In *Renewable Energy Forecasting*; Kariniotakis, G., Ed.; Woodhead Publishing Series in Energy, Woodhead Publishing, 2017; pp. 219 – 233. doi:<https://doi.org/10.1016/B978-0-08-100504-0-00008-1>.
7. Sørensen, P.; Cutululis, N.A.; Vigueras-Rodríguez, A.; Madsen, H.; Pinson, P.; Jensen, L.E.; Hjerrild, J.; Donovan, M. Modelling of power fluctuations from large offshore wind farms. *Wind Energy* **2008**, *11*, 29–43. doi:10.1002/we.246.
8. Akhmatov, V.; Abildgaard, H.; Pedersen, J.; Eriksen, P. Integration of Offshore Wind Power into the Western Danish Power System. *Proc. Copenhagen Offshore Wind 2005* **2005**.
9. van Kooten, G.C. Wind power: the economic impact of intermittency. *Letters in Spatial and Resource Sciences* **2010**, *3*, 1–17. doi:10.1007/s12076-009-0031-y.
10. Ela, E.; Kirby, B. ERCOT Event on February 26, 2008: Lessons Learned. Technical report, National Renewable Energy Laboratory, 2008. doi:10.2172/1218412.
11. Gallego-Castillo, C.; Cuerva-Tejero, A.; Lopez-Garcia, O. A review on the recent history of wind power ramp forecasting. *Renewable and Sustainable Energy Reviews* **2015**, *52*, 1148 – 1157. doi:10.1016/j.rser.2015.07.154.

- 915 12. Würth, I.; Ellinghaus, S.; Wigger, M.; Niemeier, M.J.; Clifton, A.; Cheng, P.W. Forecasting wind
916 ramps: can long-range lidar increase accuracy? *Journal of Physics: Conference Series* **2018**, *1102*, 012013.
917 doi:10.1088/1742-6596/1102/1/012013.
- 918 13. Schlipf, D.; Schlipf, D.J.; Kühn, M. Nonlinear model predictive control of wind turbines using LIDAR.
919 *Wind Energy* **2013**, *16*, 1107–1129. doi:10.1002/we.1533.
- 920 14. Bossanyi, E. Combining induction control and wake steering for wind farm energy and fatigue loads
921 optimisation. *J. Phys.: Conf. Ser.* **2018**, *1037*. doi:10.1088/1742-6596/1037/3/032011.
- 922 15. Momoh, J.A. *Smart grid: fundamentals of design and analysis*; Vol. 63, John Wiley & Sons, 2012.
- 923 16. Menin, M.; Uzunoglu, B. Parametric Sensitivity Study for Wind Power Trading through Stochastic Reserve
924 and Energy Market Optimization. 2015 Seventh Annual IEEE Green Technologies Conference, 2015, pp.
925 82–87. doi:10.1109/GREENTECH.2015.37.
- 926 17. Uzunoglu, B.; Bayazit, D. A generic resampling particle filter joint parameter estimation for electricity
927 prices with jump diffusion. 2013 10th International Conference on the European Energy Market (EEM),
928 2013, pp. 1–7. doi:10.1109/EEM.2013.6607409.
- 929 18. Uzunoglu, B.; AkifÜlker, M.; Bayazit, D. Particle filter joint state and parameter estimation of dynamic
930 power systems. 2016 57th International Scientific Conference on Power and Electrical Engineering of Riga
931 Technical University (RTUCON), 2016, pp. 1–7. doi:10.1109/RTUCON.2016.7763152.
- 932 19. Uzunoğlu, B.; Ülker, M.A. Maximum Likelihood Ensemble Filter State Estimation for Power Systems.
933 *IEEE Transactions on Instrumentation and Measurement* **2018**, *67*, 2097–2106. doi:10.1109/TIM.2018.2814066.
- 934 20. Ülker, M.A.; Uzunoğlu, B. Simplex optimization for particle filter joint state and parameter estimation of
935 dynamic power systems. *IEEE EUROCON 2017 -17th International Conference on Smart Technologies*,
936 2017, pp. 399–404. doi:10.1109/EUROCON.2017.8011142.
- 937 21. Eriksson, R.; Modig, N.; Elkington, K. Synthetic inertia versus fast frequency response: a definition. *IET
938 Renewable Power Generation* **2018**, *12*, 507–514. doi:10.1049/iet-rpg.2017.0370.
- 939 22. Díaz-González, F.; Haub, M.; Sumper, A.; Gomis-Bellmuntac, O. Participation of wind power plants
940 in system frequency control: Review of grid code requirements and control methods. *Renewable and
941 Sustainable Energy Reviews* **2014**, *43*, 551–564. doi:10.1016/j.rser.2014.03.040.
- 942 23. Mazzi, N.; Pinson, P. 10 - Wind power in electricity markets and the value of forecasting. In *Renewable
943 Energy Forecasting*; Kariniotakis, G., Ed.; Woodhead Publishing Series in Energy, Woodhead Publishing,
944 2017; pp. 259 – 278. doi:<https://doi.org/10.1016/B978-0-08-100504-0.00010-X>.
- 945 24. EPEX Spot SE. *Intraday Continous: Intraday Lead Times*, (accessed December 10, 2018).
- 946 25. NordPool. *Intraday Trading*, (accessed December 10, 2018).
- 947 26. Energy Exchange Istanbul (EXIST). *Intra-day Market*, (accessed December 10, 2018). <https://www.epias.com.tr/en/intra-day-market/phases>.
- 948 27. BSP South Pool. *Intraday Continous Market*, (accessed December 10, 2018). <https://www.bsp-southpool.com/intraday-continuous-market.html>.
- 949 28. Möhren, C., J.J. A new algorithm for Upscaling and Short-term forecasting of wind power using Ensemble
950 forecasts; Energynautics GmbH: Bremen, Germany, 2009.
- 951 29. 50Hertz.; Amprion.; Tennet.; TransnetBW. Leitfaden zur Präqualifikation von Windenergieanlagen zur
952 Erbringung von Minutenreserveleistung im Rahmen einer Pilotphase / Guidelines for Prequalification of
953 Wind Turbines to provide Minute Reserves during a Pilot Phase. Technical report, German Transmission
954 System Operators: Germany, German Transmission System Operators: Germany, 2016.
- 955 30. Pahlow, M.; Möhrlen, C.; Jørgensen, J., Application of cost functions for large-scale integration of wind
956 power using a multi-scheme ensemble prediction technique; Optimization Advances in Electric Power
957 Systems, NOVA Publisher NY, 2008.
- 958 31. IEC. Wind energy generation systems - Part 12-1: Power performance measurements of electricity
959 producing wind turbines. Standard, International Electrotechnical Commission, Geneva, CH, 2017.
- 960 32. Clifton, A.; Clive, P.; Gottschall, J.; Schlipf, D.; Simley, E.; Simmons, L.; Stein, D.; Trabucchi, D.; Vasiljevic,
961 N.; Würth, I. IEA Wind Task 32: Wind Lidar - Identifying and mitigating barriers to the adoption of wind
962 lidar. *Remote Sensing* **2018**, *10*, 413–433. doi:10.3390/rs10030406.
- 963 33. Emeis, S.; Harris, M.; Banta, R.M. Boundary-layer anemometry by optical remote sensing for wind energy
964 applications. *Meteorologische Zeitschrift* **2007**, *16*, 337–347. doi:10.1127/0941-2948/2007/0225.
- 965

- 967 34. Simley, E.; Pao, L.Y.; Frehlich, R.; Jonkman, B.; Kelley, N. Analysis of light detection and ranging wind
968 speed measurements for wind turbine control. *Wind Energy* **2014**, *17*, 413–433. doi:10.1002/we.1584.
- 969 35. Clifton, A.; Boquet, M.; Burin Des Roziers, E.; Westerhellweg, A.; Hofsass, M.; Klaas, T.; Vogstad, K.; Clive,
970 P.; Harris, M.; Wylie, S.; Osler, E.; Banta, B.; Choukulkar, A.; Lundquist, J.; Aitken, M. Remote Sensing
971 of Complex Flows by Doppler Wind Lidar: Issues and Preliminary Recommendations. Technical Report
972 TP-5000-64634, National Renewable Energy Laboratory, 2015.
- 973 36. Vasiljević, N.; L. M. Palma, J.M.; Angelou, N.; Carlos Matos, J.; Menke, R.; Lea, G.; Mann, J.; Courtney, M.;
974 Frölen Ribeiro, L.; M. G. C. Gomes, V.M. Perdigão 2015: methodology for atmospheric multi-Doppler lidar
975 experiments. *Atmospheric Measurement Techniques* **2017**, *10*, 3463–3483. doi:10.5194/amt-10-3463-2017.
- 976 37. Courtney, M.; Simon, E. *Deploying scanning lidars at coastal sites*; DTU Wind Energy: Denmark, 2016.
- 977 38. Würth, I.; Brenner, A.; Wigger, M.; Cheng, P.W. How far do we see? Analysis of the measurement range of
978 long-range lidar data for wind power forecasting. German Wind Energy Conference DEWEK, 2017.
- 979 39. Valdecabres, L.; Peña, A.; Courtney, M.; von Bremen, L.; Kühn, M. Very short-term forecast of near-coastal
980 flow using scanning lidars. *Wind Energy Science* **2018**, *3*, 313–327. doi:10.5194/wes-3-313-2018.
- 981 40. Simon, E.; Courtney, M.; Vasiljevic, N. Minute-Scale Wind Speed Forecasting Using Scanning Lidar Inflow
982 Measurements. *Wind Energy Science Discussions* **2018**. doi:10.5194/wes-2018-71.
- 983 41. Kokhanovsky, A. *Aerosol Optics: Light Absorption and Scattering by Particles in the Atmosphere*; Springer-Verlag
984 Berlin Heidelberg, 2008.
- 985 42. Performance Verification of Galion. Technical Report Report 13001, Deutsche Windguard, 2013.
- 986 43. Bradley, S. Wind speed errors for LIDARs and SODARs in complex terrain. *IOP Conference Series: Earth
987 and Environmental Science* **2008**, *1*, 012061.
- 988 44. Bradley, S.; Perrott, Y.; Behrens, P.; Oldroyd, A. Corrections for wind-speed errors from Sodar and Lidar in
989 complex terrain. *Boundary-Layer Meteorology* **2012**, *143*, 37–48. doi:10.1007/s10546-012-9702-0.
- 990 45. Bradley, S.; von Hünerbein, S.; Mikkelsen, T. A bistatic Sodar for precision wind profiling in complex
991 terrain. *Journal of Atmospheric and Oceanic Technology* **2012**, *29*, 1052–1061. doi:10.1175/JTECH-D-11-00035.1.
- 992 46. Emeis, S.; Harris, M.; Banta, R.M. Boundary-layer anemometry by optical remote sensing for wind energy
993 applications. *Meteorologische Zeitschrift* **2007**, *16*, 337–347. doi:10.1127/0941-2948/2007/0225.
- 994 47. Kindler, D.; Oldroyd, A.; MacAskill, A.; Finch, D. An eight month test campaign of the Qinetiq ZephIR
995 system: Preliminary results. *Meteorologische Zeitschrift* **2007**, *16*, 479–489. doi:10.1127/0941-2948/2007/0226.
- 996 48. Yang, Q.; Berg, L.; Pekour, M.; Fast, J.; Newsom, R. Evaluation of WRF-Predicted Near-Hub-Height Winds
997 and Ramp Events over a Pacific Northwest Site with Complex Terrain. *J. of Appl. Meteo. and Climatology*
998 **2013**, *52*, 1753–1763. doi:10.1175/JAMC-D-12-0267.1.
- 999 49. Clifton, A.; M.Boquet.; Burin, E.; Hofst  , M.; Klaas, T.; Vogstad, K.; Clive, P.; Harris, M.; Wylie, S.; E.Osler.;
1000 Banta, R.; Choukulkar, A.; Lundquist, J.; Aitken., M. Remote Sensing of Complex Flows by Doppler
1001 Wind Lidar: Issues and Preliminary Recommendations. Technical report, National Renewable Energy
1002 Laboratory, 15013 Denver West Parkway, Golden, CO 80401, 2015.
- 1003 50. Vasiljević, N.; L. M. Palma, J.M.; Angelou, N.; Carlos Matos, J.; Menke, R.; Lea, G.; Mann, J.; Courtney, M.;
1004 Fr  len Ribeiro, L.; M. G. C. Gomes, V.M. Perdig  o 2015: methodology for atmospheric multi-Doppler lidar
1005 experiments. *Atmospheric Measurement Techniques* **2017**, *10*, 3463–3483. doi:10.5194/amt-10-3463-2017.
- 1006 51. Wulfmeyer, V.; Turner, D.D.; Baker, B.; Banta, R.; Behrendt, A.; Bonin, T.; Brewer, W.A.; Buban, M.;
1007 Choukulkar, A.; Dumas, E.; Hardesty, R.M.; Heus, T.; Ingwersen, J.; Lange, D.; Lee, T.R.;
1008 Metzendorf, S.; Muppa, S.K.; Meyers, T.; Newsom, R.; Osman, M.; Raasch, S.; Santanello, J.; Senff, C.;
1009 Sp  th, F.; Wagner, T.; Weckwerth, T. A New Research Approach for Observing and Characterizing
1010 Land-Atmosphere Feedback. *Bulletin of the American Meteorological Society* **2018**, *99*, 1639–1667,
1011 [https://doi.org/10.1175/BAMS-D-17-0009.1]. doi:10.1175/BAMS-D-17-0009.1.
- 1012 52. Hirth, B.D.; Schroeder, J.L.; Gunter, W.S.; Guynes, J.G. Measuring a Utility-Scale Turbine Wake Using
1013 the TTUKa Mobile Research Radars. *Journal of Atmospheric and Oceanic Technology* **2012**, *29*, 765–771.
1014 doi:10.1175/JTECH-D-12-00039.1.
- 1015 53. Hirth, B.D.; Schroeder, J.L.; Gunter, W.S.; Guynes, J.G. Coupling Doppler radar-derived wind maps
1016 with operational turbine data to document wind farm complex flows. *Wind Energy* **2015**, *18*, 529–540.
1017 doi:10.1002/we.1701.
- 1018 54. Nygaard, N.G.; Newcombe, A.C. Wake behind an offshore wind farm observed with dual-Doppler radars.
1019 *Journal of Physics: Conference Series* **2018**, *1037*, 072008. doi:10.1088/1742-6596/1037/7/072008.

- 1020 55. Marathe, N.; Swift, A.; Hirth, B.; Walker, R.; Schroeder, J. Characterizing power performance and wake of
1021 a wind turbine under yaw and blade pitch. *Wind Energy* **2016**, *19*, 963–978. doi:10.1002/we.1875.
- 1022 56. Hirth, B.D.; Schroeder, J.L.; Irons, Z.; Walter, K. Dual-Doppler measurements of a wind ramp event at an
1023 Oklahoma wind plant. *Wind Energy* **2016**, *19*, 953–962. doi:10.1002/we.1867.
- 1024 57. Valldecabres, L.; Nygaard, N.G.; Vera-Tudela, L.; von Bremen, L.; Kühn, M. On the Use of
1025 Dual-Doppler Radar Measurements for Very Short-Term Wind Power Forecasts. *Remote Sensing* **2018**, *10*.
1026 doi:10.3390/rs10111701.
- 1027 58. Trombe, P.J.; Pinson, P.; Vincent, C.; Bøvith, T.; Cutululis, N.A.; Draxl, C.; Giebel, G.; N.Hahmann, A.;
1028 E.Jensen, N.; Jensen, B.P.; Le, N.F.; Madsen, H.; Pedersen, L.B.; Sommer, A. Weather radars – the new eyes
1029 for offshore wind farms? *Wind Energy* **2014**, *17*, 1767–1787. doi:10.1002/we.1659.
- 1030 59. Freedman, J.M.; Manobianco, J.; Schroeder, J.; Ancell, B.; Brewster, K.; Basu, S.; Banunarayanan, V.;
1031 Hodge, B.M.; Flores, I. The Wind Forecast Improvement Project (WFIP): A Public/Private Partnership for
1032 Improving Short Term Wind Energy Forecasts and Quantifying the Benefits of Utility Operations. The
1033 Southern Study Area, Final Report **2014**. doi:10.2172/1129905.
- 1034 60. *Meteorological Assimilation Data Ingest System (MADIS)*, (accessed December 10, 2018).
- 1035 61. Wilczak, J.; Finley, C.; Freedman, J.; Cline, J.; Bianco, L.; Olson, J.; Djalalova, I.; Sheridan, L.; Ahlstrom,
1036 M.; Manobianco, J.; Zack, J.; Carley, J.R.; Benjamin, S.; Coulter, R.; Berg, L.K.; Mirocha, J.; Clawson, K.;
1037 Natenberg, E.; Marquis, M. The Wind Forecast Improvement Project (WFIP): A Public–Private Partnership
1038 Addressing Wind Energy Forecast Needs. *Bull. Amer. Meteor. Soc.* **2015**, *96*, 1699–1718.
- 1039 62. Nakafuji, D. Distributed Resource Energy Analysis & Management System (DREAMS) Development for
1040 Real-time Grid Operations. Technical Report DOE-EE0006331-FTR1, Hawaiian Electric Company to U.S.
1041 Department of Energy, 2016.
- 1042 63. Pinson, P. Very-short-term probabilistic forecasting of wind power with generalized logit–normal
1043 distributions. *Journal of the Royal Statistical Society: Series C (Applied Statistics)* **2012**, *61*, 555–576.
1044 doi:10.1111/j.1467-9876.2011.01026.x.
- 1045 64. Torres, J.; García, A.; Blas, M.D.; Francisco, A.D. Forecast of hourly average wind speed with ARMA models
1046 in Navarre (Spain). *Solar Energy* **2005**, *79*, 65 – 77. doi:<https://doi.org/10.1016/j.solener.2004.09.013>.
- 1047 65. Erdem, E.; Shi, J. ARMA based approaches for forecasting the tuple of wind speed and direction. *Applied
1048 Energy* **2011**, *88*, 1405 – 1414. doi:<https://doi.org/10.1016/j.apenergy.2010.10.031>.
- 1049 66. Li, G.; Shi, J. On comparing three artificial neural networks for wind speed forecasting. *Applied Energy*
1050 **2010**, *87*, 2313 – 2320. doi:<https://doi.org/10.1016/j.apenergy.2009.12.013>.
- 1051 67. Feng, C.; Cui, M.; Hodge, B.M.; Zhang, J. A data-driven multi-model methodology with
1052 deep feature selection for short-term wind forecasting. *Applied Energy* **2017**, *190*, 1245 – 1257.
1053 doi:<https://doi.org/10.1016/j.apenergy.2017.01.043>.
- 1054 68. Niu, T.; Wang, J.; Zhang, K.; Du, P. Multi-step-ahead wind speed forecasting based on optimal feature
1055 selection and a modified bat algorithm with the cognition strategy. *Renewable Energy* **2018**, *118*, 213–229.
1056 doi:10.1016/j.renene.2017.10.075.
- 1057 69. Pinson, P. Introducing distributed learning approaches in wind power forecasting. 2016
1058 International Conference on Probabilistic Methods Applied to Power Systems (PMAPS), 2016, pp. 1–6.
1059 doi:10.1109/PMAPS.2016.7764224.
- 1060 70. Hochreiter, S.; Schmidhuber, J. Long Short-Term Memory. *Neural Computation* **1997**, *9*, 1735–1780.
1061 doi:10.1162/neco.1997.9.8.1735.
- 1062 71. Wu, W.; Chen, K.; Qiao, Y.; Lu, Z. Probabilistic short-term wind power forecasting based on deep neural
1063 networks. 2016 International Conference on Probabilistic Methods Applied to Power Systems (PMAPS),
1064 2016, pp. 1–8. doi:10.1109/PMAPS.2016.7764155.
- 1065 72. Ailliot, P.; Monbet, V. Markov-switching autoregressive models for wind time series. *Environmental
1066 Modelling & Software* **2012**, *30*, 92 – 101. doi:<https://doi.org/10.1016/j.envsoft.2011.10.011>.
- 1067 73. Pinson, P.; Madsen, H. Adaptive modelling and forecasting of offshore wind power fluctuations with
1068 Markov-switching autoregressive models. *Journal of Forecasting* **2012**, *31*, 281–313. doi:10.1002/for.1194.
- 1069 74. Browell, J.; Drew, D.R.; Philippopoulos, K. Improved very short-term spatio-temporal wind forecasting
1070 using atmospheric regimes. *Wind Energy* **2018**, *0*. doi:10.1002/we.2207.

- 1071 75. Browell, J.; Gilbert, C. Cluster-based regime-switching AR for the EEM 2017 Wind Power Forecasting
1072 Competition. 2017 14th International Conference on the European Energy Market (EEM), 2017, pp. 1–6.
1073 doi:10.1109/EEM.2017.7982034.
- 1074 76. Trombe, P.; Pinson, P.; Madsen, H. Automatic Classification of Offshore Wind Regimes With Weather
1075 Radar Observations. *IEEE Journal of Selected Topics in Applied Earth Observations and Remote Sensing* **2014**,
1076 7, 116–125. doi:10.1109/JSTARS.2013.2252604.
- 1077 77. Hering, A.S.; Genton, M.G. Powering Up With Space-Time Wind Forecasting. *Journal of the American
1078 Statistical Association* **2010**, 105, 92–104. doi:10.1198/jasa.2009.ap08117.
- 1079 78. Dowell, J.; Pinson, P. Very-Short-Term Probabilistic Wind Power Forecasts by Sparse Vector Autoregression.
1080 *IEEE Transactions on Smart Grid* **2016**, 7, 763–770. doi:10.1109/TSG.2015.2424078.
- 1081 79. Messner, J.W.; Pinson, P. Online adaptive lasso estimation in vector autoregressive models
1082 for high dimensional wind power forecasting. *International Journal of Forecasting* **2018**.
1083 doi:<https://doi.org/10.1016/j.ijforecast.2018.02.001>.
- 1084 80. Cavalcante, L.; Bessa, R.J.; Reis, M.; Browell, J. LASSO vector autoregression structures for very short-term
1085 wind power forecasting. *Wind Energy* **2017**, 20, 657–675. doi:10.1002/we.2029.
- 1086 81. Zhang, Y.; Wang, J.; Wang, X. Review on probabilistic forecasting of wind power generation. *Renewable and
1087 Sustainable Energy Reviews* **2014**, 32, 255–270. doi:10.1016/j.rser.2014.01.033.
- 1088 82. Dowell, J.; Pinson, P. Very-Short-Term Probabilistic Wind Power Forecasts by Sparse Vector Autoregression.
1089 *IEEE Transactions on Smart Grid* **2016**, 7, 763–770. doi:10.1109/TSG.2015.2424078.
- 1090 83. Jeon, J.; Taylor, J.W. Using Conditional Kernel Density Estimation for Wind Power Density Forecasting.
1091 *Journal of the American Statistical Association* **2012**, 107, 66–79. doi:10.1080/01621459.2011.643745.
- 1092 84. Wan, C.; Xu, Z.; Pinson, P.; Dong, Z.Y.; Wong, K.P. Probabilistic Forecasting of Wind Power
1093 Generation Using Extreme Learning Machine. *IEEE Transactions on Power Systems* **2014**, 29, 1033–1044.
1094 doi:10.1109/TPWRS.2013.2287871.
- 1095 85. Bessa, R.J.; Möhrlein, C.; Fundel, V.; Siefert, M.; Browell, J.; Haglund El Gaidi, S.; Hodge, B.M.; Cali, U.;
1096 Kariniotakis, G. Towards Improved Understanding of the Applicability of Uncertainty Forecasts in the
1097 Electric Power Industry. *Energies* **2017**, 10. doi:10.3390/en10091402.
- 1098 86. Yıldırım, N.; Uzunoğlu, B. Data Mining via Association Rules for Power Ramps Detected by Clustering or
1099 Optimization. In *Transactions on Computational Science XXVIII: Special Issue on Cyberworlds and Cybersecurity*;
1100 Springer Berlin Heidelberg: Berlin, Heidelberg, 2016; pp. 163–176. doi:10.1007/978-3-662-53090-0_9.
- 1101 87. Yıldırım, N.; Uzunoğlu, B. Spatial Clustering for Temporal Power Ramp Balance and Wind Power
1102 Estimation. 2015 Seventh Annual IEEE Green Technologies Conference, 2015, pp. 214–220.
1103 doi:10.1109/GREENTECH.2015.39.
- 1104 88. Yıldırım, N.; Uzunoğlu, B. Association Rules for Clustering Algorithms for Data Mining of Temporal
1105 Power Ramp Balance. 2015 International Conference on Cyberworlds (CW), 2015, pp. 224–228.
1106 doi:10.1109/CW.2015.72.
- 1107 89. Dey, C. Evolution of objective analysis methods of NMC's Medium-Range Model. *Wea. Forecasting* **1989**,
1108 4, 391–400.
- 1109 90. Ide, K.; Courtier, P.; Ghil, M.; Lorenc, A.C. Unified Notation for Data Assimilation: Operational, Sequential
1110 and Variational. *Journal of the Meteorological Society of Japan. Ser. II, Special Issue on Data Assimilation in
1111 Meteorology and Oceanography: Theory and practice* **1997**, 75, 181–189. doi:10.2151/jmsj1965.75.1B_181.
- 1112 91. Cressman, G.P. An operational objective analysis system. *Monthly Weather Review* **1959**, 87, 367–374.
1113 doi:10.1175/1520-0493(1959)087<0367:AOOAS>2.0.CO;2.
- 1114 92. Gandin, L., Objective Analysis of meteorological fields; Gidromet, English translation Jerusalem: Israel
1115 program for scientific translation, 1965.
- 1116 93. Kanamitsu, M. Description of the NMC Global Data Assimilation and Forecast System. *Weather and
1117 Forecasting* **1989**, 4, 335–342. doi:10.1175/1520-0434(1989)004<0335:DOTNGD>2.0.CO;2.
- 1118 94. Courtier, P.; Andersson, E.; Heckley, W.; Vasiljevic, D.; Hamrud, M.; Hollingsworth, A.; Rabier, F.;
1119 Fisher, M.; Pailleux, J. The ECMWF implementation of three-dimensional variational assimilation
(3D-Var). I: Formulation. *Quarterly Journal of the Royal Meteorological Society* **1998**, 124, 1783–1807.
1120 doi:10.1002/qj.49712455002.
- 1121

- 1122 95. Wu, W.S.; Purser, R.J.; Parrish, D.F. Three-Dimensional Variational Analysis with
1123 Spatially Inhomogeneous Covariances. *Monthly Weather Review* **2002**, *130*, 2905–2916.
1124 doi:10.1175/1520-0493(2002)130<2905:TDVAWS>2.0.CO;2.
- 1125 96. Courtier, P.; Thépaut, J.N.; Hollingsworth, A. A strategy for operational implementation of 4D-Var,
1126 using an incremental approach. *Quarterly Journal of the Royal Meteorological Society* **1994**, *120*, 1367–1387.
1127 doi:10.1002/qj.49712051912.
- 1128 97. Zupanski, D. A General Weak Constraint Applicable to Operational 4DVAR Data Assimilation Systems.
1129 *Monthly Weather Review* **1997**, *125*, 2274–2292. doi:10.1175/1520-0493(1997)125<2274:AGWCAT>2.0.CO;2.
- 1130 98. Kalmann, R.; Bucy, R.S. New Results in Linear Filtering and Prediction Theory. *ASME. J. Basic Eng.* **1961**,
1131 *83*, 95–108. doi:10.1115/1.3658902.
- 1132 99. Jazwinski, A. *Stochastic Processes and Filtering Theory*; Mathematics in Science and Engineering, Elsevier
1133 Science, 1970.
- 1134 100. Ristic, B.; Arulampalm, S.; Gordon, N. *Beyond the Kalman filter: particle filters for tracking applications*; The
1135 Artech House radar library, Artech House, Incorporated, 2004.
- 1136 101. Evensen, G. Sequential data assimilation with a nonlinear quasi-geostrophic model using Monte Carlo
1137 methods to forecast error statistics. *Journal of Geophysical Research: Oceans* **1994**, *99*, 10143–10162.
1138 doi:10.1029/94JC00572.
- 1139 102. Todling, R.; Cohn, S.E.; Sivakumaran, N.S. Suboptimal Schemes for Retrospective Data Assimilation
1140 Based on the Fixed-Lag Kalman Smoother. *Monthly Weather Review* **1998**, *126*, 2274–2286.
1141 doi:10.1175/1520-0493(1998)126<2274:SSFRDA>2.0.CO;2.
- 1142 103. Anderson, J.L. An Ensemble Adjustment Kalman Filter for Data Assimilation. *Monthly Weather Review*
1143 **2001**, *129*, 2884–2903. doi:10.1175/1520-0493(2001)129<2884:AEAKFF>2.0.CO;2.
- 1144 104. Houtekamer, P.L.; Mitchell, H.L. A Sequential Ensemble Kalman Filter for Atmospheric Data Assimilation.
1145 *Monthly Weather Review* **2001**, *129*, 123–137. doi:10.1175/1520-0493(2001)129<0123:ASEKFF>2.0.CO;2.
- 1146 105. Meng, Z.; Zhang, F. Tests of an Ensemble Kalman Filter for Mesoscale and Regional-Scale Data
1147 Assimilation. Part II: Imperfect Model Experiments. *Monthly Weather Review* **2007**, *135*, 1403–1423.
1148 doi:10.1175/MWR3352.1.
- 1149 106. Möhrken, C. Uncertainty in wind energy forecasting. PhD thesis, National University of Ireland, Cork,
1150 Ireland, 2004.
- 1151 107. Xiong, X.; Navon, I.M.; Uzunoglu, B. A Note on the Particle Filter with Posterior Gaussian Resampling.
1152 *Tellus A: Dynamic Meteorology and Oceanography* **2006**, *58*, 456–460. doi:10.1111/j.1600-0870.2006.00185.x.
- 1153 108. Uzunoglu, B.; Fletcher, S.J.; Zupanski, M.; Navon, I.M. Adaptive ensemble reduction and inflation.
1154 *Quarterly Journal of the Royal Meteorological Society* **2007**, *133*, 1281–1294. doi:10.1002/qj.96.
- 1155 109. Zupanski, M. Maximum Likelihood Ensemble Filter: Theoretical Aspects. *Monthly Weather Review* **2005**,
1156 *133*, 1710–1726. doi:10.1175/MWR2946.1.
- 1157 110. Houtekamer, P.L.; Mitchell, H.L.; Pellerin, G.; Buehner, M.; Charron, M.; Spacek, L.; Hansen, B. Atmospheric
1158 Data Assimilation with an Ensemble Kalman Filter: Results with Real Observations. *Monthly Weather Review*
1159 **2005**, *133*, 604–620. doi:10.1175/MWR-2864.1.
- 1160 111. Hamill, T.M.; Snyder, C. Using Improved Background-Error Covariances from an Ensemble
1161 Kalman Filter for Adaptive Observations. *Monthly Weather Review* **2002**, *130*, 1552–1572.
1162 doi:10.1175/1520-0493(2002)130<1552:UIBECF>2.0.CO;2.
- 1163 112. Snyder, C.; Zhang, F. Assimilation of Simulated Doppler Radar Observations with an Ensemble Kalman
1164 Filter. *Monthly Weather Review* **2003**, *131*, 1663–1677. doi:10.1175//2555.1.
- 1165 113. Zhang, F.; Snyder, C.; Sun, J. Impacts of Initial Estimate and Observation Availability on Convective-Scale
1166 Data Assimilation with an Ensemble Kalman Filter. *Monthly Weather Review* **2004**, *132*, 1238–1253.
1167 doi:10.1175/1520-0493(2004)132<1238:IOIEAO>2.0.CO;2.
- 1168 114. DISPATCH. Technical report, Australien Electricity Market Operator (AEMO), Level 22, 530 Collins Street
1169 Melbourne VIC 3000, Australia, 2018.
- 1170 115. Borup, L. IEA Wind Task 36 Forecasting webinar: How to run 40% RE in the Danish system.
1171 <https://www.youtube.com/watch?v=IGhUasWctUM>, last accessed 3. 12. 2018, 2018.
- 1172 116. Germany, B. *EEG in Zahlen 2016*, 2016.

¹¹⁷³ © 2019 by the authors. Submitted to *Energies* for possible open access publication under the terms and conditions
¹¹⁷⁴ of the Creative Commons Attribution (CC BY) license (<http://creativecommons.org/licenses/by/4.0/>).